Published for SISSA by Springer

Received: *January 19, 2023*
Accepted: *April 3, 2023*
Published: *June 12, 2023*

Search for top squarks in the four-body decay mode with single lepton final states in proton-proton collisions at $\sqrt{s} = 13$ TeV

The CMS collaboration

E-mail: cms-publication-committee-chair@cern.ch

Abstract: A search for the pair production of the lightest supersymmetric partner of the top quark, the top squark ($\tilde{t}_1$), is presented. The search targets the four-body decay of the $\tilde{t}_1$, which is preferred when the mass difference between the top squark and the lightest supersymmetric particle is smaller than the mass of the W boson. This decay mode consists of a bottom quark, two other fermions, and the lightest neutralino ($\tilde{\chi}_1^0$), which is assumed to be the lightest supersymmetric particle. The data correspond to an integrated luminosity of 138 fb^{-1} of proton-proton collisions at a center-of-mass energy of 13 TeV collected by the CMS experiment at the CERN LHC. Events are selected using the presence of a high-momentum jet, an electron or muon with low transverse momentum, and a significant missing transverse momentum. The signal is selected based on a multivariate approach that is optimized for the difference between $m(\tilde{t}_1)$ and $m(\tilde{\chi}_1^0)$. The contribution from leading background processes is estimated from data. No significant excess is observed above the expectation from standard model processes. The results of this search exclude top squarks at 95% confidence level for masses up to 480 and 700 GeV for $m(\tilde{t}_1) - m(\tilde{\chi}_1^0) = 10$ and 80 GeV, respectively.

Keywords: Hadron-Hadron Scattering , Supersymmetry, Top Squark

ArXiv ePrint: 2301.08096

https://doi.org/10.1007/JHEP06(2023)060

JHEP06(2023)060

Contents

JHEP06(2023)060

1 Introduction

Supersymmetry (SUSY) [1–6] predicts the existence of a new symmetry that requires that, for each fermion (boson) in the standard model (SM), there is also a bosonic (fermionic) superpartner. Searches for SUSY are among the important focal points of the physics program at the CERN LHC, since SUSY naturally solves the problem of quadratically divergent loop corrections to the mass of the Higgs boson [7–9]. If R parity [10] is conserved, supersymmetric particles would be produced in pairs, and their decay chains would end with the lightest supersymmetric particle (LSP), often considered to be the lightest neutralino $\widetilde{\chi}_1^0$. Such an LSP, being neutral, weakly interacting, and massive, would have the required characteristics for a dark matter particle, and thus, would offer a solution to another shortcoming of the SM. When the symmetry is broken, the scalar partners of an SM fermion acquire a mass different from the mass of the SM partner, with the mass splitting between scalar mass eigenstates being proportional to the mass of the SM fermion. Since the top quark is the heaviest fermion of the SM, the splitting between its chiral supersymmetric partners can be the largest among all supersymmetric quarks (squarks). Furthermore, the

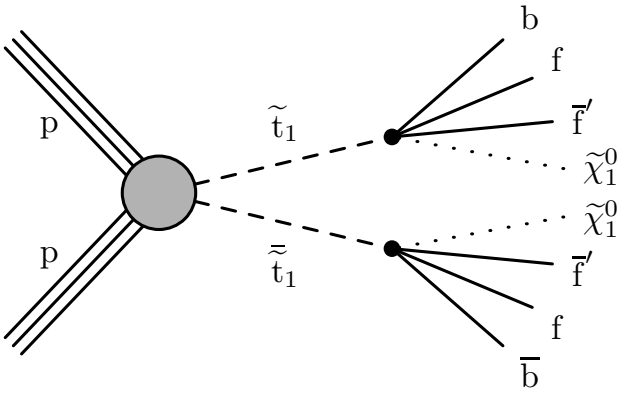

Figure 1. Diagram of top squark pair production $\widetilde{\mathrm{t}}_1\overline{\widetilde{\mathrm{t}}}_1$ in pp collisions, with a four-body decay of each top squark.

top Yukawa coupling can be the greatest among all fermions, which affects the masses of the squarks through the renormalization group equations. The lighter supersymmetric scalar partner of the top quark, the top squark ($\widetilde{\mathrm{t}}_1$), could therefore be the lightest squark. If SUSY is realized in nature, cosmological observations imply that for many models the lightest top squark should be almost degenerate with the LSP [11]. In this scenario, because the mass difference between the $\widetilde{\mathrm{t}}_1$ and the $\widetilde{\chi}_1^0$ is smaller than the mass of the W boson, the two- and three-body decays of the $\widetilde{\mathrm{t}}_1$ are kinematically forbidden, while the two-body decay to $\mathrm{c}\widetilde{\chi}_1^0$ can be suppressed depending on the parameters of the model. This motivates the search for the four-body decay $\widetilde{\mathrm{t}}_1 \to \mathrm{bf}\overline{\mathrm{f}}'\widetilde{\chi}_1^0$, where b stands for the bottom quark, and the fermions f and $\overline{\mathrm{f}}'$ can be either quarks or leptons. Throughout this paper, charge conjugation is assumed. Figure 1 represents a simplified model [12–17] of the production of $\widetilde{\mathrm{t}}_1\overline{\widetilde{\mathrm{t}}}_1$ in proton-proton (pp) collisions, where each $\widetilde{\mathrm{t}}_1$ and $\overline{\widetilde{\mathrm{t}}}_1$ undergoes a four-body decay.

In this paper, the previous 2016 result of CMS at $\sqrt{s} = 13\,\mathrm{TeV}$ [18] is combined with data recorded in 2017 and 2018. The results of 2016 are directly taken from ref. [18], except the integrated luminosity and its uncertainty, which are updated to their latest values [19]. The total integrated luminosity for the combined 2016–2018 analysis is $138\,\mathrm{fb}^{-1}$.

In the present search a final state is considered, where the fermions f and $\overline{\mathrm{f}}'$ represent a charged lepton and its neutrino for the decay products of one $\widetilde{\mathrm{t}}_1$, and two quarks for the other top squark. A 100% branching fraction is assumed for the four-body decay when interpreting the results [12]. The considered final states contain at least one jet, a large missing transverse momentum, and exactly one charged lepton, which can be either an electron or a muon. The choice of final states where one top squark decays into a lepton is motivated by the decrease of the contributions from the multijet background in this mode, while increasing the selection efficiency with the other top squark decaying hadronically. The selected jet, attributed to initial-state radiation (ISR) of a parton, is required to have high transverse momentum (p_T). Both neutralinos and the neutrino escape undetected, leaving high missing transverse momentum. Electrons and muons can

JHEP06(2023)060

be efficiently reconstructed and identified with p_{T} as low as 5.0 and 3.5 GeV, respectively. The signal selection is based on a multivariate analysis, followed by a counting experiment. This approach takes advantage of the different correlations between the discriminating variables for signal and background, and is adapted for different $\Delta m = m(\tilde{\mathrm{t}}_1) - m(\tilde{\chi}_1^0)$ kinematic regions, thus enhancing the reach of the search across the $(m(\tilde{\mathrm{t}}_1),\ m(\tilde{\chi}_1^0))$ space. The main contributions to the background events are W+jets, $\mathrm{t\bar{t}}$, and Z+jets processes, and are predicted from data. A search in the single-lepton final state for the four-body decays of the $\tilde{\mathrm{t}}_1$ has been performed by the ATLAS Collaboration at $\sqrt{s} = 13$ TeV [20], and a comparison of its results to the present search is provided in this paper. Tabulated results are provided in the HEPData record for this search [21].

2 The CMS detector

The central feature of the CMS apparatus [22] is a superconducting solenoid of 6 m internal diameter, providing a magnetic field of 3.8 T. Within the solenoid volume are a silicon pixel and strip tracker, a lead tungstate crystal electromagnetic calorimeter (ECAL), and a brass and scintillator hadron calorimeter (HCAL), each composed of a barrel and two endcap sections. Forward calorimeters extend the pseudorapidity coverage provided by the barrel and endcap detectors. The silicon tracker measures charged particles within the pseudorapidity range $|\eta| < 2.5$. Muons are detected in gas-ionization chambers embedded in the steel flux-return yoke outside the solenoid. It is a multipurpose, nearly hermetic detector, designed to trigger on [23, 24] and identify electrons, muons, photons, and hadrons [25–27].

3 Data and simulated samples

The search described in this paper is performed using data from pp collisions recorded in 2017–2018 by the CMS experiment at the LHC at a center-of-mass energy of 13 TeV. These results are statistically combined with the result from the search using the data of 2016, corresponding to an integrated luminosity of 36.3 fb^{-1} that was updated for this paper. The 2017 and 2018 data samples correspond to an integrated luminosity of 41.5 fb^{-1} and 59.8 fb^{-1}, respectively, bringing the total integrated luminosity for the combined 2016–2018 analysis to 138 fb^{-1}.

Signal and background processes are simulated using several Monte Carlo (MC) event generators. The SM background MC samples are used to estimate the relation between the control and signal regions for the main background processes, to validate the background estimation methods based on control samples in data, and finally, to predict the contributions from other processes. The W+jets, $\mathrm{Z} \to \nu\bar{\nu}$+jets, and multijet processes are generated at leading order (LO) by MadGraph5_aMC@NLO 2.4.2 [28]. The $\mathrm{t\bar{t}}$ process is generated at next-to-leading order (NLO) by MadGraph5_aMC@NLO. The POWHEG v2.0 [29–36] generators are used for the NLO simulations of single top and associated tW production. Diboson events are simulated at NLO with MadGraph5_aMC@NLO and POWHEG. The LO (NLO) NNPDF3.1LO (NNPDF3.1NLO) [37] parton distribution functions are used

JHEP06(2023)060

consistently with the order of the matrix element calculation in the generated events. Additional backgrounds such as $\mathrm{t\bar{t}}$ produced in association with a Z boson, W boson, or photon, referred to as $\mathrm{t\bar{t}X}$, are generated with MadGraph5_aMC@NLO at NLO [38]. Hadronization and showering of events in all generated samples are simulated using Pythia 8.230 [39] with the CP5 tune [40] for the underlying event. All SM MC events are passed through a full simulation of the CMS apparatus, where the response of the detector is modeled using the Geant4 [41] software. Generated events are processed using the same version of the CMS event reconstruction software used as for data. Additional pp collisions in the same or nearby beam crossings (pileup) are simulated and overlaid on the main pp interaction in the MC samples, with distributions that reproduce the conditions observed year-to-year in data. For the pair production of top squarks ($\widetilde{\mathrm{t}}_1\bar{\widetilde{\mathrm{t}}}_1$), simulated samples are produced for $250 < m(\widetilde{\mathrm{t}}_1) < 800\,\mathrm{GeV}$ in steps of 25 GeV, and $10 < \Delta m < 80\,\mathrm{GeV}$ in steps of 10 GeV. The cross section for $\widetilde{\mathrm{t}}_1\bar{\widetilde{\mathrm{t}}}_1$ production, calculated using Prospino v.2 [42–48], is computed at next-to-next-to-leading-order (NNLO) accuracy, and includes next-to-next-to-leading-logarithmic (NNLL) corrections [49, 50]. This cross section varies between approximately 25 and 0.03 pb as $\mathrm{m}(\widetilde{\mathrm{t}}_1)$ goes from 250 to 800 GeV. The generation of signal events with up to two additional jets, which can originate from ISR, is performed with MadGraph5_aMC@NLO and then interfaced with Pythia for the decay hadronization and showering. The modeling of the detector response for the signal is done with the CMS fast simulation program [51, 52]. The simulated samples of all background processes are used to check the modeling of variables at the preselection level (see section 5.1). For the final results, the yields of W+jets, $\mathrm{t\bar{t}}$, $\mathrm{Z} \to \nu\bar{\nu}$+jets and multijet backgrounds, as well as the associated systematic uncertainties, are predicted using data-driven techniques (see sections 6 and 7).

Both signal and background simulated samples are corrected to account for discrepancies from data. Control regions (CRs) in data are used to measure the reconstruction efficiencies of leptons and jets produced by the hadronization of b quarks, "b jets", as well as the b jet misidentification probabilities for light-quark and gluon jets. The corrections are applied as a function of the p_{T} and η of the objects. Fast simulation signal samples are additionally corrected to take into account any potential difference with respect to the Geant4 modeling. The latter corrections translate into efficiencies applied to b jets, leptons, and the modeling of the missing transverse momentum. The simulations of W+jets, $\mathrm{t\bar{t}}$, and signal processes are corrected for the effect of ISR. The modeling of ISR for these processes is checked in data-based control samples that are highly enriched in $\mathrm{t\bar{t}}$ or W+jets events. The simulation of $\mathrm{t\bar{t}}$ events is tested by comparing the jet multiplicity observed in a control sample with the simulation, and the $\mathrm{t\bar{t}}$ and signal samples are reweighted based on this comparison. The simulation of W+jets events is corrected based on the distribution of the sum of the magnitudes of the lepton ℓ transverse momentum $p_{\mathrm{T}}(\ell)$ and the missing transverse momentum in a control sample.

JHEP06(2023)060

4 Event reconstruction and object selection

Data and simulated events are reconstructed using the CMS particle-flow (PF) algorithm [53], which matches the information from all CMS subdetectors in order to describe the event in terms of global physics objects. These objects are denoted as PF candidates and are classified into mutually exclusive categories: electrons, muons, photons, and charged and neutral hadrons. The primary vertex (PV) is taken to be the vertex corresponding to the hardest scattering in the event, evaluated using tracking information alone, as described in section 9.4.1 of ref. [54].

Jets are reconstructed by applying the anti-k_{T} clustering algorithm [55, 56] to PF candidates with a distance parameter of 0.4. The pileup contribution to the jet momentum is partially taken into account by excluding the charged hadrons originating from vertices other than the PV from the jet-clustering algorithm. To account for pileup contributions from neutral particles and any inhomogeneity in the detector response, the jet p_{T} is further calibrated as described in ref. [57]. Jets are required to satisfy $p_{\mathrm{T}} > 30\,\mathrm{GeV}$, and $|\eta| < 2.4$. The tagging of b jets (b tagging) is performed with the DeepCSV algorithm [58] that uses information from the secondary vertex and is based on a deep neural network. The b tagging discriminant is used to tag jets as b jets based on a set of working points (loose, medium, tight) and to define further event variables based on the discriminant value or the jet with highest discriminant value. The b jet identification working points are defined as the selection values in the discriminator distribution at which the probability of misidentifying a light-flavor jet as a b jet is 10%, 1% and 0.1%, respectively, for the loose, medium and tight working points [59].

The missing transverse momentum vector, $\vec{p}_{\mathrm{T}}^{\,\mathrm{miss}}$, is computed as the negative vector $\vec{p_{\mathrm{T}}}$ sum of all PF candidates in the event, and its magnitude is $p_{\mathrm{T}}^{\mathrm{miss}}$. The calibrations associated with the jet energy estimations are propagated to the $\vec{p}_{\mathrm{T}}^{\,\mathrm{miss}}$ [60].

Electron candidates are reconstructed from energy deposits in the ECAL and matched charged particle tracks in the inner tracker obtained using the Gaussian sum filter algorithm [25]. To reduce the number of misidentified electrons, additional constraints on the shape of the electromagnetic shower in the ECAL, the quality of the match between the trajectory of the track, and the ECAL energy deposit around the electron, and the relative HCAL deposit in the electron direction are applied. Electrons are required to have p_{T} above 5 GeV and $|\eta| < 2.5$, with a veto on electron candidates in the ECAL gap region ($1.4442 < |\eta| < 1.5660$). They are identified with requirements on the observables that describe the matching of the measurements in the tracker and the ECAL, the description of energy clusters in the ECAL, and the amount of bremsstrahlung radiation emitted during the propagation through the detector. A loose working point of this algorithm is required for electrons to be selected, which has an average efficiency of 90%.

Muon candidates are reconstructed by combining the information from the silicon tracking systems and the muon spectrometer in a global fit [26] that assigns a quality to the matching between the tracker and muon systems and imposes minimal requirements on the track to reduce the misidentification of muons. The medium working point of this algorithm is required for muons to be selected, which ensures an efficiency above 98%. Muons are required to pass the selection requirements of $p_{\mathrm{T}} > 3.5\,\mathrm{GeV}$ and $|\eta| < 2.4$.

JHEP06(2023)060

To select electrons or muons originating from the PV, the point of closest approach of the associated track with respect to the PV is required to have a transverse distance $|d_{xy}| < 0.02\,\text{cm}$, and a longitudinal distance $|d_z| < 0.1\,\text{cm}$. A lepton is defined as being nonprompt either when it does not originate from the PV, or when a jet is misidentified as a lepton. Background processes with nonprompt leptons are one of the main contributions to the SM background in the signal regions. In this analysis, nonprompt leptons mostly arise from heavy-quark decays in jets produced in association with a $\mathrm{Z} \to \nu\bar{\nu}$+jets decay, from multijet production, or from W+jets and $\mathrm{t\bar{t}}$ events where the prompt lepton was not reconstructed and a different one was accepted. In order to suppress these types of processes, a requirement on the lepton isolation is applied, which uses a combination of an absolute and a relative isolation variable. The absolute isolation variable I_{abs} of the lepton is defined as the scalar sum of the p_{T} of PF candidates within a cone size of $R \equiv \sqrt{(\Delta\phi)^2 + (\Delta\eta)^2} = 0.3$, where ϕ is the azimuthal angle, around the lepton candidate, which is excluded from the sum, as are charged PF candidates not associated with the PV. The contributions from neutral particles originating from pileup are estimated according to the method described in refs. [61, 62], and are subtracted from I_{abs}. The ratio of the lepton I_{abs} to the lepton p_{T} is defined as the lepton relative isolation I_{rel}. A uniform lepton selection efficiency as a function of p_{T} is achieved by requiring leptons to have $I_{\text{abs}} < 5\,\text{GeV}$ for $p_{\mathrm{T}}(\ell) < 25\,\text{GeV}$ and $I_{\text{rel}} < 0.2$ for $p_{\mathrm{T}}(\ell) \geq 25\,\text{GeV}$.

5 Event selection

The data events collected by the trigger system are required to have both $p_{\mathrm{T}}^{\text{miss}}$ and $H_{\mathrm{T}}^{\text{miss}}$ above 120 GeV, where $H_{\mathrm{T}}^{\text{miss}}$ is the magnitude of the missing transverse momentum calculated only from jets. In order to maintain the performance of the online selection with increased luminosity from the late runs of 2017 onward, the condition $H_{\mathrm{T}} > 60\,\text{GeV}$ is also required, where H_{T} is defined as the scalar p_{T} sum of all jets in the event. The efficiency of the combined $p_{\mathrm{T}}^{\text{miss}}$ and $H_{\mathrm{T}}^{\text{miss}}$ trigger is measured using an independent event sample with single-electron triggers and p_{T} thresholds of 35 and 32 GeV for the 2017 and 2018 data-taking periods, respectively.

The offline event selection is a two-step process. First, a preselection is applied to reduce the contribution of the main background processes (section 5.1) by selecting a single charged lepton, large $p_{\mathrm{T}}^{\text{miss}}$, and jets. Then, boosted decision trees (BDTs) [63, 64] are trained and used to define the signal selection (section 5.2). The preselection is constructed to be as inclusive as possible in order to maintain a high signal efficiency for all Δm values, leaving the main selection to the BDT.

5.1 Preselection

The value of the preselection $p_{\mathrm{T}}^{\text{miss}}$ threshold is set close to the beginning of the maximum efficiency plateau of the combined $p_{\mathrm{T}}^{\text{miss}}$ and $H_{\mathrm{T}}^{\text{miss}}$ trigger, while optimizing the separation between signal and background performed by the BDTs. Events with $p_{\mathrm{T}}^{\text{miss}} > 280\,\text{GeV}$ are selected, favoring the signal where two $\tilde{\chi}_1^0$'s escape detection and where the $p_{\mathrm{T}}^{\text{miss}}$ is therefore larger than for SM processes. For these events, the trigger efficiency is above 98%

JHEP06(2023)060

for both years. To account for the small inefficiency, simulated samples are reweighted as a function of $p_{\mathrm{T}}^{\mathrm{miss}}$ to match the efficiency of the triggers in data.

To suppress the contribution of SM processes, additional requirements are imposed on the selected events. In particular, to reduce the W+jets background, $H_{\mathrm{T}} > 200\,\mathrm{GeV}$ is required. To select the single-lepton topology, it is demanded exactly one identified electron or muon in the event, along with at least one jet. This selection reduces the contribution from the dilepton topology of $\mathrm{t\bar{t}}$ events. To further improve the selection of signal over SM background events, at least one jet must have $p_{\mathrm{T}} > 110\,\mathrm{GeV}$. These requirements are geared towards signal events in which the $\tilde{\mathrm{t}}_1\bar{\tilde{\mathrm{t}}}_1$ system recoils against a high-momentum ISR jet, Lorentz boosting the $\tilde{\chi}_1^0$ and increasing $p_{\mathrm{T}}^{\mathrm{miss}}$. The ISR jet will often be the highest momentum (leading) jet in these events, and the leading-jet p_{T} threshold value is optimized in the same manner as for $p_{\mathrm{T}}^{\mathrm{miss}}$. Lastly, in events with at least two jets, the azimuthal angle between the directions of the leading and second-highest-p_{T} (subleading) jets must be smaller than 2.5 radians, suppressing the SM multijet background.

After the preselection, the W+jets and $\mathrm{t\bar{t}}$ processes are the main SM backgrounds, making up about 70 and 20%, respectively, of the total expected background. The $\mathrm{Z} \to \nu\bar{\nu}$+jets process contributes to the SM background by having jets, genuine $p_{\mathrm{T}}^{\mathrm{miss}}$, and a jet misidentified as a lepton. The remaining background processes are diboson, single top quark, Drell-Yan (DY), multijet, and $\mathrm{t\bar{t}X}$ production where X is a vector boson. These processes are a less-important part of the expected background because of having a smaller cross section, a lower acceptance, or both. The $p_{\mathrm{T}}(\ell)$, $p_{\mathrm{T}}^{\mathrm{miss}}$, and N_{jet} distributions after the preselection from the 2017 and 2018 data and the simulations are shown in figure 2, where N_{jet} is the number of jets in the event satisfying the jet criteria. The simulated background distributions for each year are normalized to the corresponding integrated luminosity. The level of agreement with data gives us confidence in training the BDTs with the simulated distributions for the second step in the event selection.

5.2 Classification and final selection

The selection of the signal events is based on a BDT [64] to take advantage of the different correlations among the discriminating variables for the signal and background processes. For each event passing the preselection, the BDT discriminator value, henceforth referred to as the BDT output, is evaluated. If the discriminator value exceeds the determined threshold, the event is retained. The choice of the discriminating variables used as input to the BDT is made by maximizing a figure of merit (FOM) [65] that takes into account the statistical and systematic uncertainties in a selection. Various BDTs are trained with different sets of discriminating variables, and a variable is included in the final set only if it significantly increases the FOM obtained for any selection using the BDT output. The list of the twelve retained input variables and a short description of their signal and background distributions is as follows:

- Variables related to $p_{\mathrm{T}}^{\mathrm{miss}}$: $p_{\mathrm{T}}^{\mathrm{miss}}$ and m_{T} , where m_{T} is the transverse mass of the lepton + $\vec{p}_{\mathrm{T}}^{\,\mathrm{miss}}$ system, defined as: $m_{\mathrm{T}} = \sqrt{2p_{\mathrm{T}}^{\ell}p_{\mathrm{T}}^{\mathrm{miss}}[1-\cos(\Delta\phi_{\ell,\vec{p}_{\mathrm{T}}^{\,\mathrm{miss}}})]}$, where $\Delta\phi$ is the azimuthal angular difference between the lepton $\vec{p}_{\mathrm{T}}$ and $\vec{p}_{\mathrm{T}}^{\,\mathrm{miss}}$. The $p_{\mathrm{T}}^{\mathrm{miss}}$

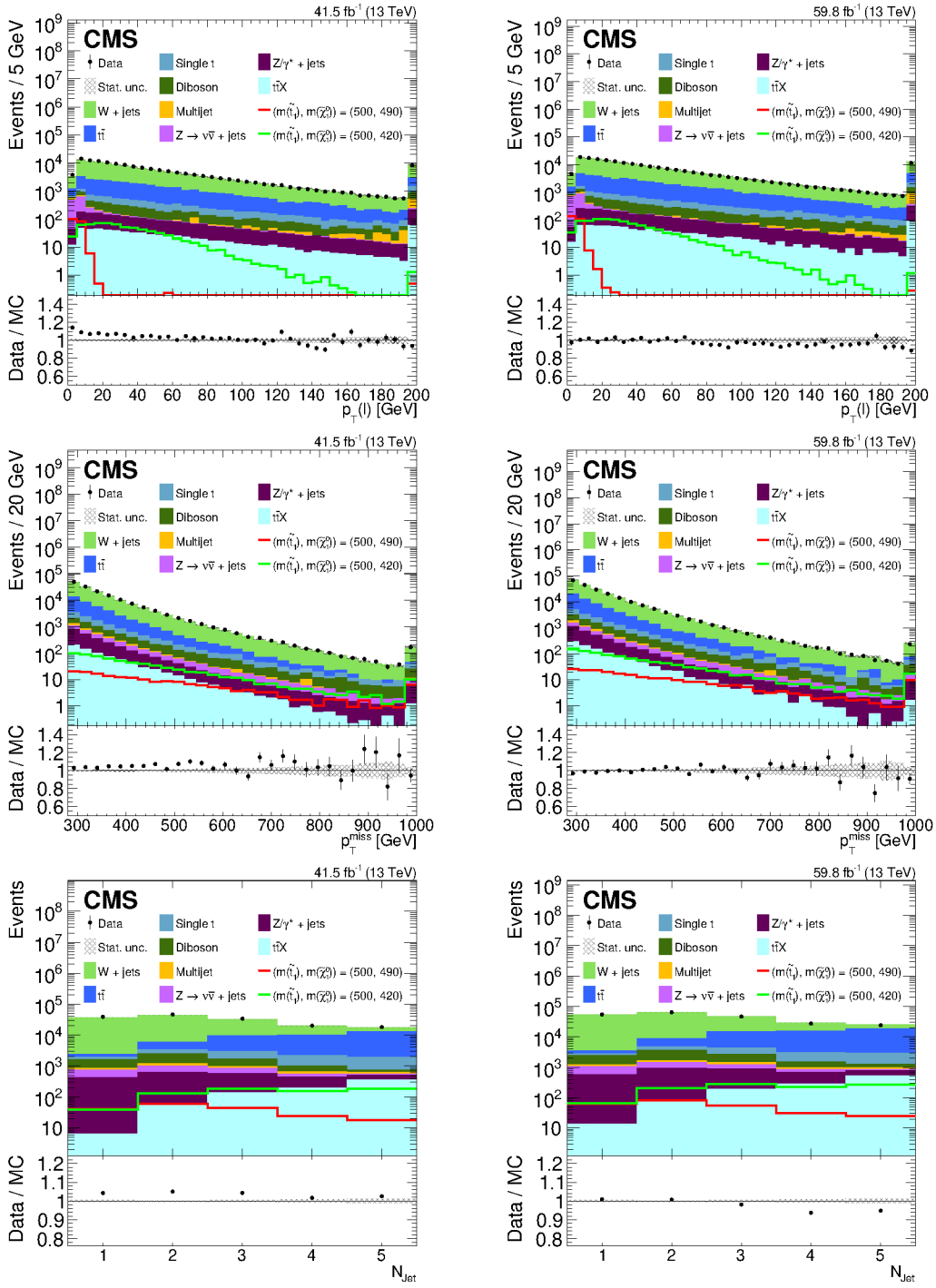

Figure 2. Distributions of $p_{\mathrm{T}}(\ell)$ (upper), $p_{\mathrm{T}}^{\mathrm{miss}}$ (middle), and N_{jet} (lower), after the preselection from 2017 (left) and 2018 (right) data (points) and simulation (colored histograms). The simulated distribution of two signal points are represented by colored lines, while not being stacked on the background distributions: $(m(\tilde{\mathrm{t}}_1),\ m(\tilde{\chi}_1^0)) = (500,\ 490)$ and $(500,\ 420)$ GeV. The last bin in each plot includes the overflow events. The lower panels show the ratio of data to the sum of the simulated SM backgrounds. The shaded bands indicate only the statistical uncertainty in the simulation predictions.

JHEP06(2023)060

distribution extends to higher values for the signal than for the backgrounds due to the two undetected LSPs in the signal decays. The m_{T} spectrum peaks around 80 GeV for the SM background and is a broad distribution for the signal.

- Lepton-related variables: $p_{\mathrm{T}}(\ell)$, $\eta(\ell)$, and $Q(\ell)$. The correlations between $p_{\mathrm{T}}^{\mathrm{miss}}$ and $p_{\mathrm{T}}(\ell)$ are different for the signal, where $p_{\mathrm{T}}^{\mathrm{miss}}$ comes from three undetected particles (two $\widetilde{\chi}_1^0$ and a ν), than for W+jets and $\mathrm{t\bar{t}}$ backgrounds, where $p_{\mathrm{T}}^{\mathrm{miss}}$ is the result of a single undetected particle (ν). Because the decay products of the signal are more centrally produced than those of the W+jets process, the lepton pseudorapidity $\eta(\ell)$ distribution is populated at more central values for the signal than this background. The lepton charge $Q(\ell)$ is a discriminating variable because W^+ and W^- bosons are not produced equally at the LHC, while the signal events contain equal numbers of positively and negatively charged leptons.

- Jet-related variables: $p_{\mathrm{T}}(\mathrm{ISR})$, $p_{\mathrm{T}}(\mathrm{b})$, N_{jet}, and H_{T}. The variable $p_{\mathrm{T}}(\mathrm{ISR})$ is defined as the p_{T} of the leading jet, and selects the high-momentum ISR jet in signal events. The $p_{\mathrm{T}}(\mathrm{b})$ variable is the transverse momentum of the jet with the highest b tagging discriminant value. Both the $p_{\mathrm{T}}(\mathrm{ISR})$ and $p_{\mathrm{T}}(\mathrm{b})$ variables are sensitive to the available phase space, which depends on $m(\widetilde{\mathrm{t}}_1) - m(\widetilde{\chi}_1^0)$ for the signal, and $m(\mathrm{t}) - m(\mathrm{W})$ for the $\mathrm{t\bar{t}}$ background. The N_{jet} variable is sensitive to the mass difference Δm, while the H_{T} variable provides discrimination between signal and both the W+jets and $\mathrm{t\bar{t}}$ backgrounds.

- b jet-related variables: $N(\mathrm{b}^{\mathrm{loose}})$, $\Delta R(\ell, \mathrm{b})$, and $D(\mathrm{b})$. The number of loosely b tagged jets $N(\mathrm{b}^{\mathrm{loose}})$, the distance in $(\eta,\ \phi)$ space between the directions of the lepton and the jet with the highest b tagging discriminant $\Delta R(\ell, \mathrm{b})$, and the highest b tagging discriminant per event $D(\mathrm{b})$ are included as input variables. While the preselection has no requirement on b tagging, information related to it is passed to the BDT to help discriminate between the signal and mainly the W+jets background.

The five most discriminating variables, in decreasing power, are $p_{\mathrm{T}}(\ell)$, $p_{\mathrm{T}}^{\mathrm{miss}}$, $p_{\mathrm{T}}(\mathrm{ISR})$, H_{T}, and m_{T} .

The discrimination power of the input variables varies as a function of Δm, as illustrated in figure 3 (left). An important feature of this search is the adaptation of the selection tool to the evolving kinematic variables of the signal over the $(m(\widetilde{\mathrm{t}}_1),\ m(\widetilde{\chi}_1^0))$ plane. Therefore, this plane is divided into eight Δm regions (from 10 to 80 GeV, in steps of 10), and a separate BDT is trained for each Δm region. The BDTs are trained to discriminate signal from background using the binomial log-likelihood loss function. Only the W+jets and $\mathrm{t\bar{t}}$ processes, which constitute a large fraction of the total background after preselection, are included in the training. They are normalized in proportion to their theoretical cross sections. As seen in figure 3 (right), different signal points with the same Δm have similar input variable distributions. This is expected since with the same Δm they have the same available phase space. Because of this, all the signal points with the same Δm are grouped together when training the BDT, thus increasing the number of signal

JHEP06(2023)060

events for each training. Because of the large variation of the $p_{\mathrm{T}}(\ell)$ spectrum across the $(m(\widetilde{\mathrm{t}}_1),\ m(\widetilde{\chi}_1^0))$ plane, $p_{\mathrm{T}}(\ell) < 30\,\mathrm{GeV}$ is required for $\Delta m < 70\,\mathrm{GeV}$ signal regions before training the BDTs, while imposing no restriction on $p_{\mathrm{T}}(\ell)$ for signal regions with higher Δm. This improves the ability of the BDT to separate the signal from the $\mathrm{t\bar{t}}$ background.

The BDT output distributions for data and simulated SM background are shown in figures 4 and 5 for the 2017 and 2018 data, respectively. In each case a $(m(\widetilde{\mathrm{t}}_1),\ m(\widetilde{\chi}_1^0))$ signal point belonging to the Δm value for which the training has been done is also reported. The BDT output is found to be different for various values of Δm, which is to be expected because of the changing mix of signal and background and the varying correlations across the $(m(\widetilde{\mathrm{t}}_1),\ m(\widetilde{\chi}_1^0))$ plane, resulting in different BDT outputs for different Δm values. A good agreement between the data and simulation is observed for the BDT output distributions over the entire range, for all trainings; the region at small BDT output values (e.g., <0.3) is dominated by background events.

To check the validity of the BDT output in regions depleted in signal, a set of validation regions (VRs) are defined. These regions are chosen to be kinematically close but nonoverlapping with the region selected by the preselection, while using the same online selection. The first VR uses the preselection requirements discussed in section 5.1, but where $200 < p_{\mathrm{T}}^{\mathrm{miss}} < 280\,\mathrm{GeV}$ is required. This VR is used to validate the BDT output for all the trained BDTs. The second VR also uses the preselection requirements, but where $p_{\mathrm{T}}(\ell) > 30\,\mathrm{GeV}$ is required. It is used for the validation of BDTs trained for signals with $\Delta m < 70\,\mathrm{GeV}$. This region is not used for BDTs trained for signals with $\Delta m = 70$ or 80 GeV because the entire range of the $p_{\mathrm{T}}(\ell)$ distribution is considered at preselection. The BDT output distributions for these VRs from data are consistent with those from the simulation. Figure 6 illustrates for both years the $p_{\mathrm{T}}(\ell)$ distribution for the VR where $200 < p_{\mathrm{T}}^{\mathrm{miss}} < 280\,\mathrm{GeV}$, as well as the output of the BDT for $\Delta m = 10\,\mathrm{GeV}$. Figure 7 reports for both years the $p_{\mathrm{T}}^{\mathrm{miss}}$ distribution for the VR where $p_{\mathrm{T}}(\ell) > 30\,\mathrm{GeV}$, and the output of the BDT for $\Delta m = 60\,\mathrm{GeV}$. As observed in these figures, the BDT output of data is well described by the simulation. The mismodeling of an input variable, possibly resulting in the one of the BDT output, is covered by a systematic uncertainty. As described in section 6, the VRs are used to evaluate the uncertainty in the background determination.

A signal region (SR) is defined by requiring a lower limit on each BDT output. This limit is determined by minimizing the expected upper limit on the signal cross section of a benchmark $(m(\widetilde{\mathrm{t}}_1),\ m(\widetilde{\chi}_1^0))$ signal point at the exclusion limit of the 2016 search. This choice implies that the benchmark signal points for the search from 2017 and 2018 data are at higher $\widetilde{\mathrm{t}}_1$ and $\widetilde{\chi}_1^0$ masses than for the 2016 search. The exact values of the BDT selection requirements are reported in table 2. As an illustration of the selection power of the BDT, in the case of $\Delta m = 80\,\mathrm{GeV}$, the SM background is suppressed by a factor of $\approx 3.7 \times 10^3$ compared to the preselection, while the signal is only reduced by a factor of ≈ 13.

6 Background estimation

The main background processes in this search are W+jets and $\mathrm{t\bar{t}}$, both with a prompt lepton, and events where the lepton arises from the decay of heavy-flavor quarks or from

JHEP06(2023)060

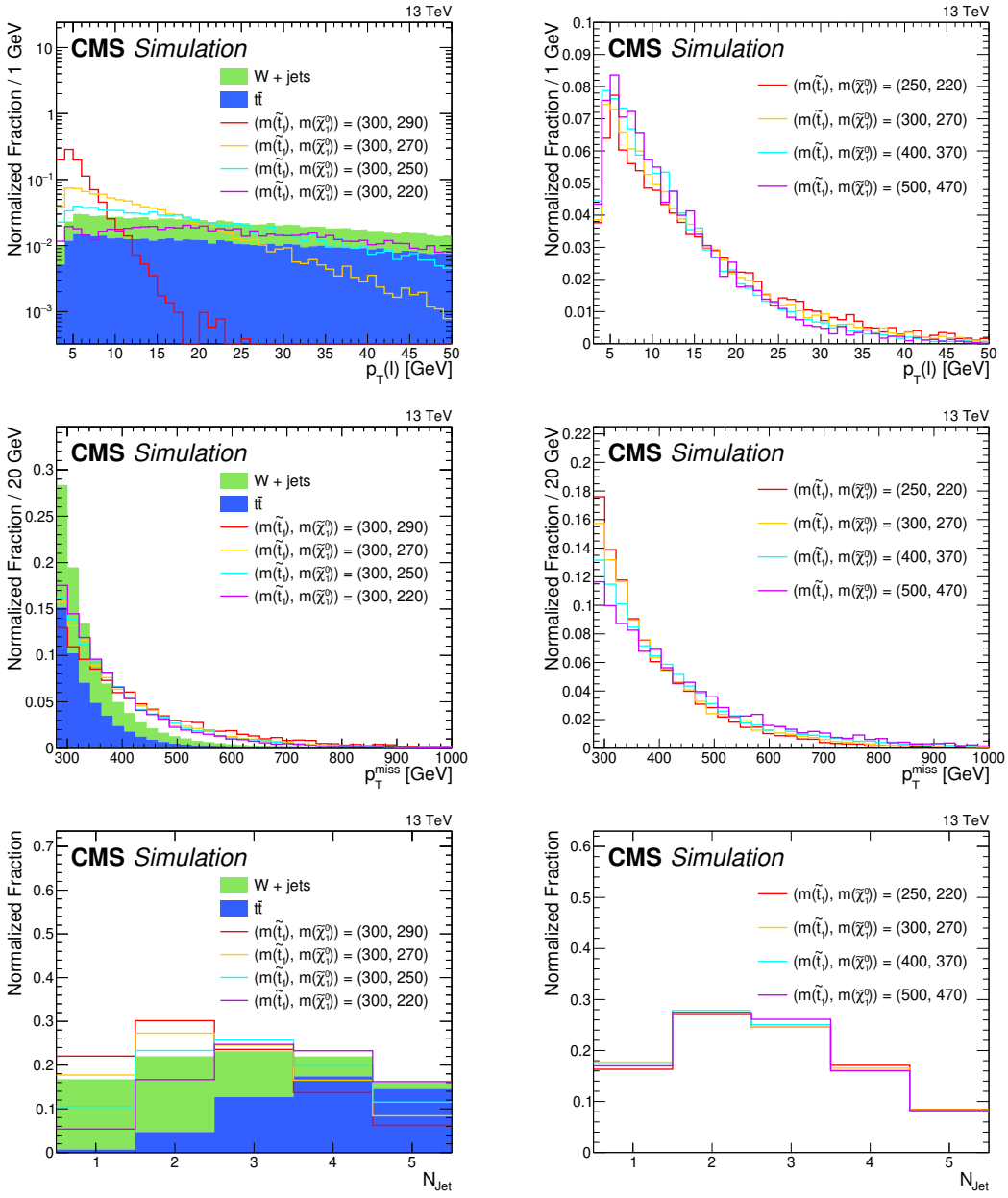

Figure 3. Simulated distributions of $p_{\mathrm{T}}(\ell)$ (upper), $p_{\mathrm{T}}^{\mathrm{miss}}$ (middle), and N_{jet} (lower) after the preselection. The W+jets and $\mathrm{t\bar{t}}$ background distributions are shown as colored histograms, and the signal distributions by the solid lines. The total background distribution and the signal distributions are all normalized to unit area. On the left, the signal distributions are given for a top squark mass of 300 GeV and $\Delta m = 10$, 30, 50, and 80 GeV. On the right, the signal distributions are shown for four different $(m(\tilde{\mathrm{t}}_1),\ m(\tilde{\chi}_1^0))$ values, all corresponding to the same $\Delta m = 30$ GeV.

JHEP06(2023)060

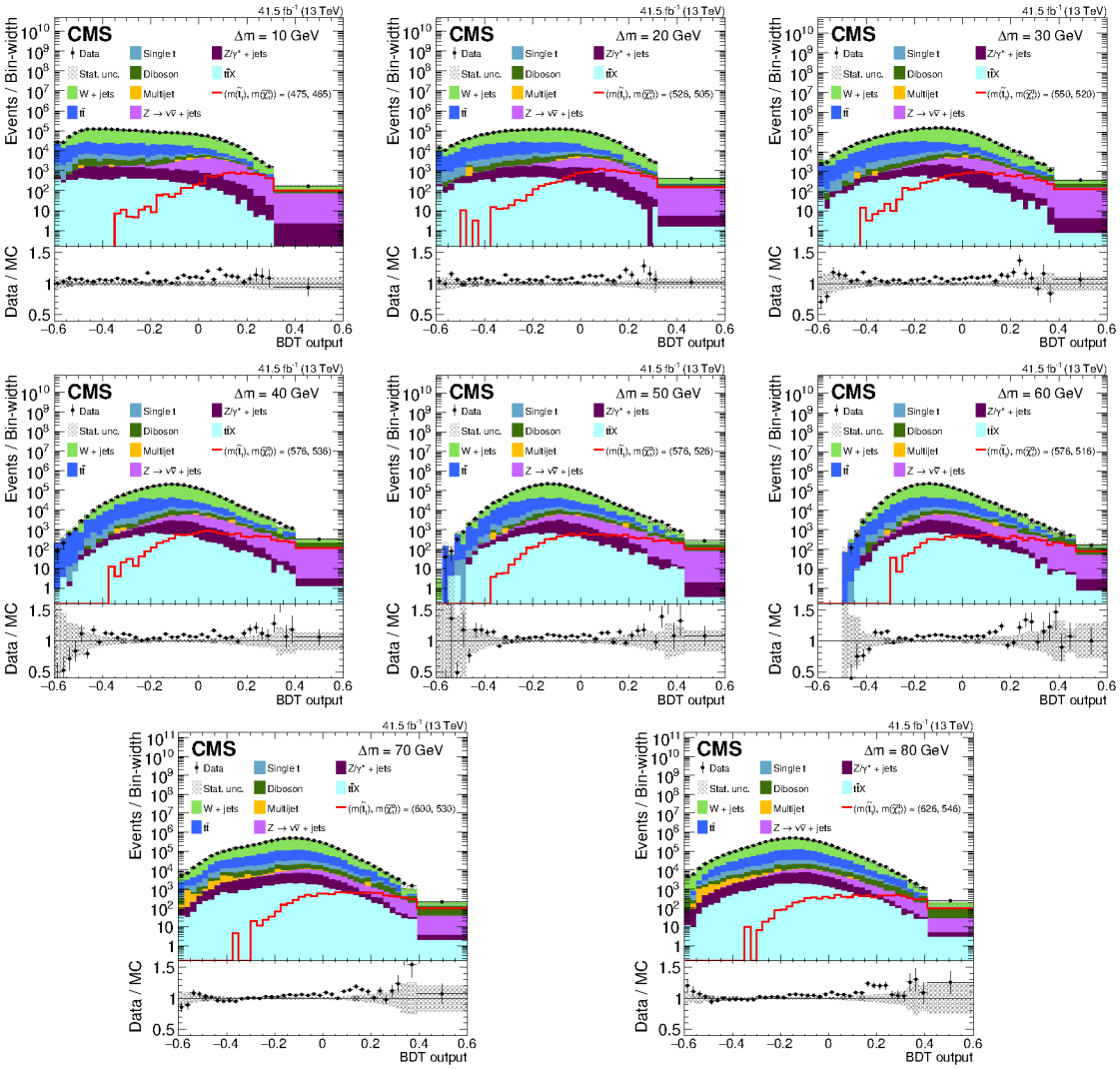

Figure 4. BDT output distributions from data (points) and simulation (colored histograms) after the preselection in 10 GeV steps of Δm from 10 (upper left) to 80 (lower right) GeV for the 2017 data. The last bin corresponds to the SR. For each Δm value, the predicted signal distribution is shown by the solid red line for a representative $(m(\widetilde{\mathrm{t}}_1),\ m(\widetilde{\chi}_1^0))$ point, unstacked from the histograms. The lower panels show the ratio of the data to the sum of the background predictions, with the vertical bars and shaded area giving only the statistical uncertainty in the data and the simulated background, respectively.

misidentified hadrons that pass the lepton criteria. The latter category is labeled as nonprompt background. The processes contributing to the nonprompt background are mainly $\mathrm{Z} \to \nu\bar{\nu}$+jets, and to a lesser extent, W+jets and $\mathrm{t\bar{t}}$, where a jet is misidentified as a lepton, as well as the multijet background. Furthermore, there can also be events in which a genuine lepton (mainly from W+jets or $\mathrm{t\bar{t}}$) escapes detection, while a nonprompt lepton is selected. These three main sources of background are estimated using data, as described in sections 6.1 and 6.2. The background from other SM processes, such as single top quark,

JHEP06(2023)060

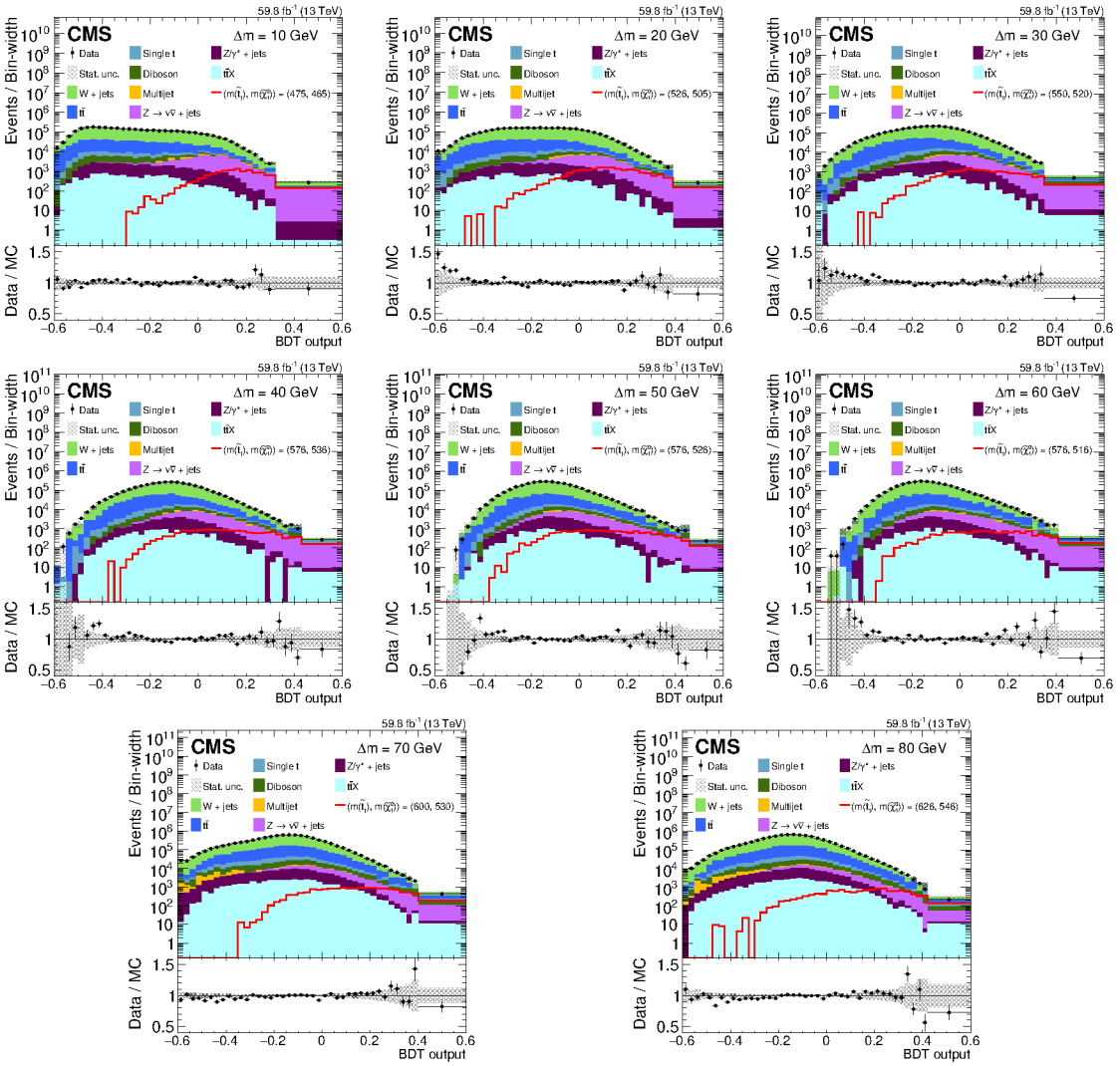

Figure 5. BDT output distributions from data (points) and simulation (colored histograms) after the preselection in 10 GeV steps of Δm from 10 (upper left) to 80 (lower right) GeV for the 2018 data. The last bin corresponds to the SR. For each Δm value, the predicted signal distribution is shown by the solid red line for a representative $(m(\tilde{t}_1),\ m(\tilde{\chi}_1^0))$ point, unstacked from the histograms. The lower panels show the ratio of the data to the sum of the background predictions, with the vertical bars and shaded area giving only the statistical uncertainty in the data and the simulated background, respectively.

diboson, DY, and $t\bar{t}X$ production, are estimated from simulation. In the following section, background yields estimated using data are denoted by Y while background yields estimated only from simulated samples are denoted by N.

6.1 Nonprompt background

The nonprompt background is estimated from data using the "tight-to-loose" method [66]. The tight criteria correspond to the selection of the lepton as described in section 4. The

JHEP06(2023)060

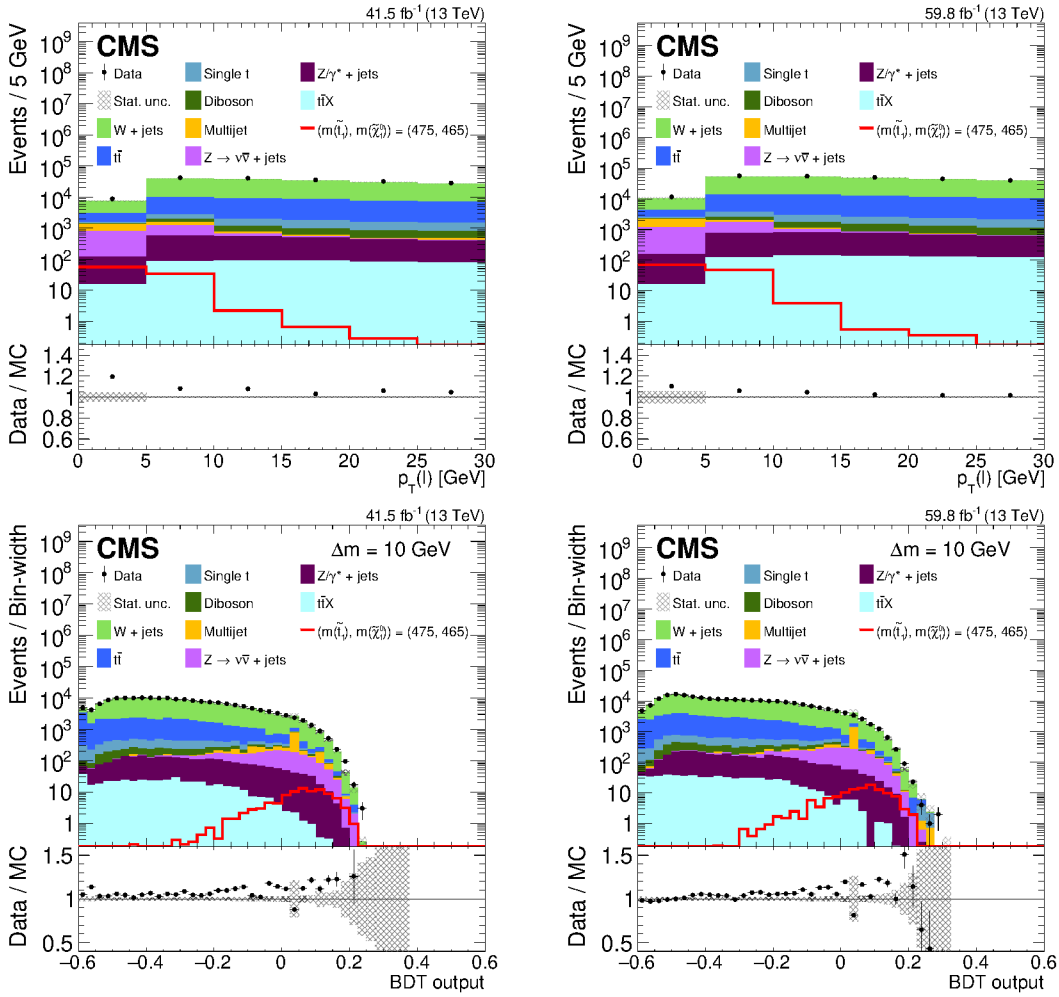

Figure 6. Distributions of $p_{\mathrm{T}}(\ell)$ (upper) and BDT output for $\Delta m = 10\,\mathrm{GeV}$ (lower) in the VR where $200 < p_{\mathrm{T}}^{\mathrm{miss}} < 280\,\mathrm{GeV}$, from 2017 (left) and 2018 (right) data (points) and simulation (colored histograms). The predicted signal distribution is shown by the solid red line for $(m(\tilde{\mathrm{t}}_1),\ m(\tilde{\chi}_1^0)) = (475, 465)$, unstacked from the histograms. The lower panels show the ratio of data to the sum of the simulated SM backgrounds. The shaded bands indicate only the statistical uncertainty in the simulation predictions.

loose selection is defined by relaxing the requirement on the isolation variable to $I_{\mathrm{abs}} < 20\,\mathrm{GeV}$ for $p_{\mathrm{T}}(\ell) < 25\,\mathrm{GeV}$ and $I_{\mathrm{rel}} < 0.8$ for $p_{\mathrm{T}}(\ell) > 25\,\mathrm{GeV}$, and on the impact parameters to $|d_{xy}| < 0.1\,\mathrm{cm}$ and $|d_z| < 0.5\,\mathrm{cm}$. A lepton passing these requirements is called a loose lepton. The probability ϵ_{TL} for a loose lepton to pass the tight criteria is measured as a function of its p_{T} and η in a data CR that is largely dominated by multijet events and enriched in nonprompt leptons. For each SR, it is defined a side-band region with the same requirements, but where the lepton must pass the loose criteria while failing the tight ones ("L!T"). The number of such events in data is denoted as $N^{L!T}(\mathrm{Data})$. The number of events $N_{\mathrm{p}}^{L!T}(\mathrm{MC})$ from simulation where a vector boson or a top quark produce a prompt lepton are subtracted from the data sample with a loose-not-tight lepton. The predicted

JHEP06(2023)060

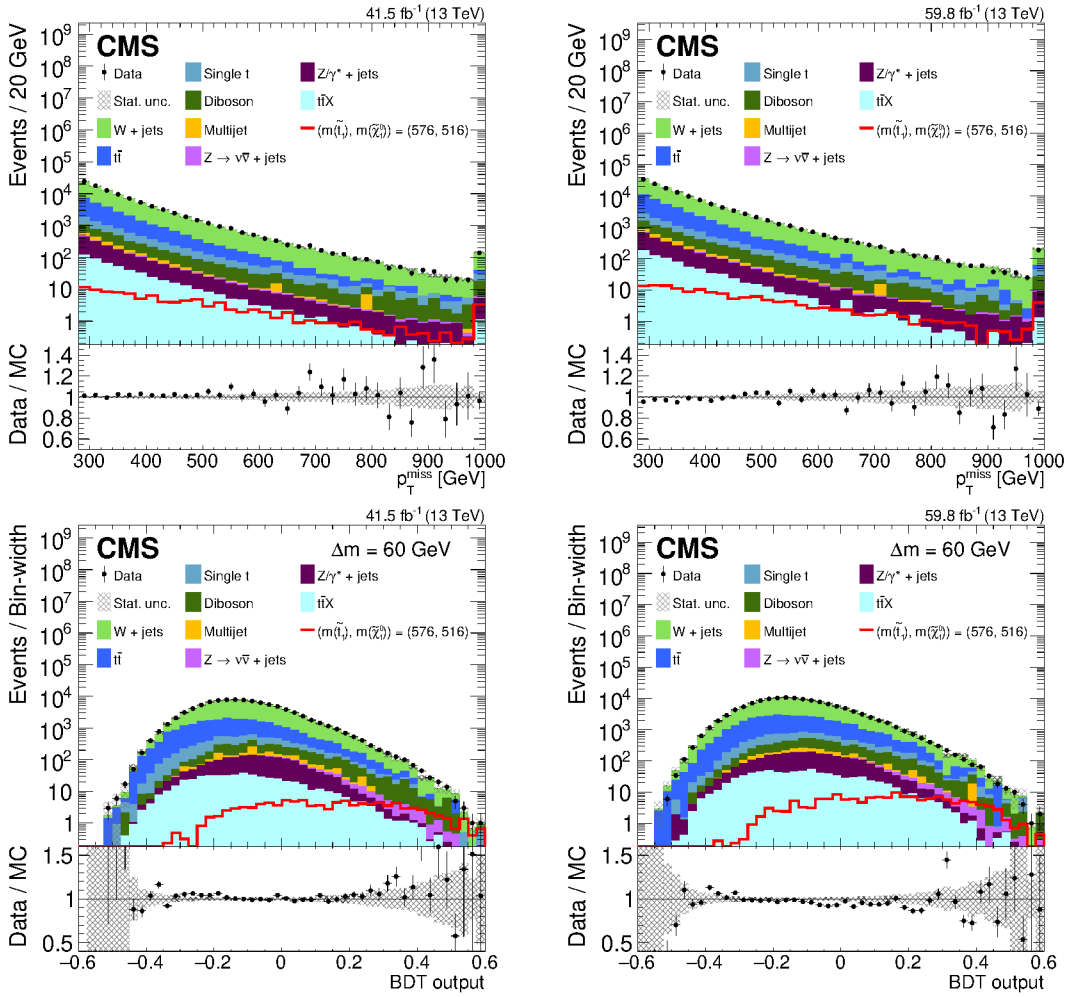

Figure 7. Distributions of $p_{\mathrm{T}}^{\mathrm{miss}}$ (upper) and BDT output for $\Delta m = 60\,\mathrm{GeV}$ (lower) in the VR where $p_{\mathrm{T}}(\ell) > 30\,\mathrm{GeV}$, from 2017 (left) and 2018 (right) data (points) and simulation (colored histograms). The predicted signal distribution is shown by the solid red line for $(m(\tilde{\mathrm{t}}_1),\ m(\tilde{\chi}_1^0)) = (576, 516)$, unstacked from the histograms. The lower panels show the ratio of data to the sum of the simulated SM backgrounds. The shaded bands indicate only the statistical uncertainty in the simulation predictions.

nonprompt yield $Y_{\mathrm{np}}^{\mathrm{SR}}$ in each SR is obtained by weighting the resulting number of events by $\epsilon_{\mathrm{TL}}/(1-\epsilon_{\mathrm{TL}})$:

$$Y_{\mathrm{np}}^{\mathrm{SR}} = \frac{\epsilon_{\mathrm{TL}}}{1-\epsilon_{\mathrm{TL}}}[N^{\mathrm{L!T}}(\mathrm{Data}) - N_{\mathrm{p}}^{\mathrm{L!T}}(\mathrm{MC})]. \tag{6.1}$$

6.2 Dominant prompt backgrounds

To estimate the prompt contributions from the W+jets and $\mathrm{t\bar{t}}$ processes, a method based on the number of these background events observed in data CRs is used. The method uses the output of the BDT, and a transfer factor between the CR and the SR, obtained from simulation. This factor, of the order 10^{-3} for both backgrounds and for both years, is the ratio of the number of predicted events in the SR, $N_{\mathrm{p}}^{\mathrm{SR}}$, to the one in the CR,

JHEP06(2023)060

$N_{\mathrm{p}}^{\mathrm{CR}}$. The estimated yield $Y_{\mathrm{p}}^{\mathrm{SR}}$ of the dominant prompt background in the SR, estimated independently per process and per year, is then determined using:

$$Y_{\mathrm{p}}^{\mathrm{SR}}(X) = \frac{N_{\mathrm{p}}^{\mathrm{SR}}(X)}{N_{\mathrm{p}}^{\mathrm{CR}}(X)} \left[N^{\mathrm{CR}}(\mathrm{Data}) - N_{\mathrm{p}}^{\mathrm{CR}}(\text{non-}X) - Y_{\mathrm{np}}^{\mathrm{CR}} \right], \tag{6.2}$$

where X refers to the background process being estimated, either W+jets or $\mathrm{t\bar{t}}$, and where the terms prompt and nonprompt refer to their definition as given at the beginning of section 6. To obtain a data sample enriched in the backgrounds being estimated, a CR is defined by applying the preselection criteria, with the additional requirement BDT < 0. The number of such events is denoted as $N^{\mathrm{CR}}(\mathrm{Data})$. To enrich the CR in W+jets or $\mathrm{t\bar{t}}$ events, the number of loosely b tagged jets is required to be zero, or the number of tightly b tagged jets to be at least one, respectively, where loose and tight were discussed in section 4 [59]. The purity of W+jets and $\mathrm{t\bar{t}}$ processes in the corresponding CRs is approximately 93% and 78%, respectively. The level of signal contamination in the CR is well below 5%. The number $N_{\mathrm{p}}^{\mathrm{CR}}(\text{non-}X)$ is the number of prompt background events other than the process being estimated in the CR, estimated from simulation and subtracted from the number of data events; e.g.: if X = W+jets, this term includes $\mathrm{t\bar{t}}$, and vice versa. The yield $Y_{\mathrm{np}}^{\mathrm{CR}}$, which is the predicted number of nonprompt background in the CR, is also subtracted.

7 Summary of systematic uncertainties

Processes for which the absolute yield is predicted by simulation are subject to systematic uncertainties in the determination of the integrated luminosity, which is estimated year-by-year with uncertainties in the 1.2–2.5% range [67, 68]. All simulated samples are subject to experimental uncertainties in the jet energy scale (JES) and jet energy resolution (JER). The uncertainties arising from miscalibration of the JES are estimated by varying the jet energy corrections up and down by one standard deviation of their uncertainties and propagating the effect to the calculation of $p_{\mathrm{T}}^{\mathrm{miss}}$. Differences in the JER between data and simulation are accounted for by smearing the momenta of jets in simulation. The uncertainties corresponding to the b tagging efficiencies and misidentification rates for tagging light-flavored quark or gluon jets as b jets have been evaluated for all simulated samples. The systematic uncertainties in the scale factors applied to the simulated samples for trigger and lepton efficiencies are taken into account. The uncertainty due to the simulation of pileup for simulated background processes is estimated by varying the inelastic pp cross section by 4.6% [69]. An uncertainty of 50% is assigned to the cross sections of all backgrounds whose yields are predicted from simulation.

The estimation of nonprompt backgrounds, as described in section 6.1, depends on the tight-to-loose fraction ϵ_{TL}, which is sensitive to the flavor content of jets. The systematic uncertainty arising from this source in the measurement region is estimated by changing the b tagging requirement in the b veto to demand at least one b tagged jet using the medium working point. The resulting uncertainty ranges from 3 to 90% from low to high lepton p_{T}, respectively. The method is also tested by repeating this procedure on the simulated

JHEP06(2023)060

event samples, where any variations in the background determination are considered as systematic uncertainties and added in quadrature to the aforementioned uncertainty.

The systematic uncertainties associated with the predictions of W+jets and $\mathrm{t\bar{t}}$ processes are based on the comparison of two methods: one to assess the closure of the background prediction method, and the other to evaluate the effect of the modeling of the BDT output distribution. The closure method measures differences between the predicted number of events (obtained from eq. (6.2)) and the observed number of data events in both VRs, as defined in section 5.2, where the statistical uncertainty in the number of CR events is taken into account. Uncertainties in modeling the BDT output distribution, which can affect the background prediction, are assessed by comparing the ratio of the BDT output distributions for data to the background prediction in the CR with the ratio in the SR, for the two VRs. To be conservative, the uncertainties are evaluated in the two VRs for both methods, and the largest value is used. These uncertainties range from 10 to 20% for the prediction of W+jets events and from 8 to 80% for the estimation of $\mathrm{t\bar{t}}$ processes over the various SRs. The estimations of the W+jets and $\mathrm{t\bar{t}}$ backgrounds rely partially on the simulation and are therefore sensitive to theoretical uncertainties in the modeling of ISR. For the $\mathrm{t\bar{t}}$ process, half of the ISR correction is assigned as the systematic uncertainty, which also applies to the simulated signal samples. For the W+jets process, the difference between the ISR-corrected and uncorrected simulation is taken as the systematic uncertainty.

Uncertainties from unknown higher-order theoretical effects are estimated through uncorrelated variations of the renormalization and factorization scales by factors of 0.5, 1, and 2 [70]. Finally, differences between the fast and the full GEANT4-based modelings of $p_{\mathrm{T}}^{\mathrm{miss}}$ are used as the corresponding systematic uncertainty and assigned to the signal yields. The statistical uncertainty in the signal simulation samples of 3 to 20% over the various SRs is included as a systematic uncertainty. The relative systematic uncertainties in the signal from the various sources, and the total relative systematic uncertainties in the W+jets, $\mathrm{t\bar{t}}$, and nonprompt backgrounds, are given in table 1 as ranges over the eight SRs.

To combine the results from the different data-taking years, systematic uncertainties whose sources are exactly the same for the different years are taken as fully correlated. This includes the uncertainty in the theoretical cross sections, pileup, JES, the reweighting of the W+jets sample, the renormalization and factorization scales, and the prediction of the W+jets, $\mathrm{t\bar{t}}$, and nonprompt backgrounds. The systematic uncertainty in the integrated luminosity has multiple components and is thus considered as partially correlated between the years [19, 67, 68], as is the systematic uncertainty in the b tagging procedure.

8 Results and interpretation

The observed and expected numbers of signal and background events from the 2017–18 data analysis for the eight values of Δm are given in table 2 and shown in figures 8 and 9. The predictions and the associated uncertainties in these figures are given before a profiled likelihood fit [71–73] is performed. The post-fit uncertainties do not get reduced because of the lack of constraints from a single bin. It should be noted that the background composition varies for the same Δm region for different years. This is because an independent

JHEP06(2023)060

	2017		2018	
Source	Background	Signal	Background	Signal
Integrated luminosity	—	2.3	—	2.5
JES	0–2	3–9	0–2	5–10
JER	0–1	0–1	0–1	0–1
b tagging	0–1	0–6	0–1	0–1
Trigger	0–1	1	0–1	1
Lepton efficiency	0–1	0–1	0–1	0–1
Pileup	1–5	0–3	1–4	0–1
ISR ($\mathrm{t\bar{t}}$ and signal)	0–1	0–5	0–1	0–5
ISR (W+jets)	0–4	—	0–4	—
Renorm./Fact. scales	0–7	0–1	0–10	0–1
$p_{\mathrm{T}}^{\mathrm{miss}}$ modeling (FastSim)	—	0–2	—	0–2
W+jets total	2–6	—	4–9	—
$\mathrm{t\bar{t}}$ total	1–5	—	2–7	—
Nonprompt lepton total	2–5	—	2–4	—

Table 1. The relative systematic uncertainties in percent from the different sources in the signal and the total relative uncertainty in the W+jets, $\mathrm{t\bar{t}}$, and nonprompt background predictions, shown separately for the 2017 and 2018 data analysis. The ranges given are across the eight SRs. The "—" symbol means that a given source of uncertainty is not applicable.

BDT is trained per Δm and per year, with a different selection on its output. There is good agreement between the observed and predicted numbers of events for all SRs. The largest difference is for $\Delta m = 10\,\mathrm{GeV}$, where there are 1.1 and 2.9 standard deviations (local significance) excesses of data events over the predicted background for the 2017 and 2018 data, respectively. The 2016 analysis had a similar excess for the same Δm value, corresponding to 0.7 standard deviations. None of these excesses is statistically significant, so it is concluded that there is no evidence for direct top squark production.

The observed and expected number of events for each signal mass point and their corresponding uncertainties are converted into 95% confidence level (CL) upper limits on the $\mathrm{\tilde{t}_1\bar{\tilde{t}}_1}$ production cross section in the $(m(\mathrm{\tilde{t}_1}),\ m(\tilde{\chi}_1^0))$ plane. These are shown by the colored regions in figure 10 as a function of $m(\mathrm{\tilde{t}_1})$ and Δm, where the color scale to the right of the figure gives the corresponding upper limit values. The limits are calculated according to the modified frequentist $\mathrm{CL_s}$ criterion [71–73]. A test statistic is defined as the likelihood ratio between the background-only and signal-plus-background hypotheses, and is used to set exclusion limits on the top squark pair production. The distributions of the test statistic are built using simulated experiments, where statistical uncertainties are modeled with Poisson distributions, and where all systematic uncertainties are modeled with a log-normal distribution. When interpreting the results, it is assumed a branching fraction of 100% for the four-body decay scenario. For the combined results of the three years, the

JHEP06(2023)060

Year	Δm (GeV)	BDT >	$Y_{\mathrm{p}}^{\mathrm{SR}}$(W+jets)	$Y_{\mathrm{p}}^{\mathrm{SR}}(\mathrm{t\bar{t}})$	$Y_{\mathrm{np}}^{\mathrm{SR}}$	N^{SR}(Other)	N^{SR}(Total)	N^{SR}(Observed)
2017	10	0.31	11.0 ± 2.4	2.2 ± 2.9	20.1 ± 3.5	5.4 ± 3.7	38.8 ± 6.3	49
	20	0.32	37.4 ± 4.6	3.3 ± 5.2	49.6 ± 7.0	18.4 ± 9.3	109 ± 14	116
	30	0.38	23.8 ± 3.8	0.0 ± 7.2	41.7 ± 6.1	19.4 ± 9.9	85 ± 14	86
	40	0.40	15.9 ± 2.6	0.0 ± 8.1	32.6 ± 5.5	20 ± 10	69 ± 15	66
	50	0.43	10.9 ± 2.0	0.0 ± 6.7	22.3 ± 4.0	17.9 ± 9.2	51 ± 12	48
	60	0.47	3.9 ± 0.8	0.0 ± 6.2	7.6 ± 2.2	10.3 ± 5.4	21.8 ± 8.5	23
	70	0.39	11.1 ± 2.0	8.9 ± 7.6	12.9 ± 2.9	19.7 ± 9.8	53 ± 13	50
	80	0.41	15.6 ± 4.3	10.3 ± 9.7	8.3 ± 2.2	17.1 ± 8.2	51 ± 14	51
2018	10	0.32	17.3 ± 4.3	0.0 ± 2.4	16.7 ± 3.6	7.1 ± 4.5	41.1 ± 7.6	77
	20	0.39	18.4 ± 2.8	0.3 ± 3.1	14.5 ± 3.4	6.3 ± 3.5	39.4 ± 6.4	57
	30	0.35	48.5 ± 8.1	9.1 ± 9.4	22.5 ± 4.8	33 ± 14	114 ± 19	127
	40	0.43	10.7 ± 3.1	3.4 ± 4.5	11.7 ± 2.9	12.3 ± 6.7	38.1 ± 9.1	49
	50	0.46	8.7 ± 3.0	3.4 ± 4.5	10.5 ± 2.8	10.3 ± 5.2	32.9 ± 8.0	36
	60	0.41	16.5 ± 4.7	16.2 ± 8.8	17.3 ± 3.8	22 ± 10	72 ± 15	61
	70	0.40	35.6 ± 8.7	15.2 ± 8.6	16.9 ± 5.2	30 ± 12	97 ± 18	96
	80	0.42	16.3 ± 3.7	10.9 ± 7.8	10.7 ± 4.3	21.5 ± 9.8	59 ± 14	41

Table 2. The predicted number of W+jets, $\mathrm{t\bar{t}}$, nonprompt, and other (N^{SR}(Other)) background events and their sum (N^{SR}(Total)), in the eight SRs for the 2017 and 2018 data analysis. The first 3 predicted yields are derived from data, while the yields of the other background processes come from simulation. The uncertainties shown are the quadratic sum of the statistical and systematic uncertainties given in table 1 for all the background processes. The corresponding Δm and BDT output threshold values for each SR are displayed in the first and second columns, respectively, and the observed number of events in data is shown in the last column.

largest excess in the data corresponds to 2.5 standard deviations (local significance) for the $\Delta m = 10\,\mathrm{GeV}$ SR.

Using the measured upper limits on the top squark pair cross section and the theoretical predictions for the cross section, it is determined the 95% CL lower limits on $m(\widetilde{\mathrm{t}}_1)$ versus Δm. The solid black line and thick dotted red line in figure 10 give the resulting 95% CL observed and expected exclusion contours, respectively, on $m(\widetilde{\mathrm{t}}_1)$ as a function of Δm, obtained from combining the 2016, 2017, and 2018 data. The corresponding thin black lines in figure 10 represent the ± 1 standard deviation (σ_{theory}) variations in the limits due to the theoretical uncertainties in the case of the observed limits. The thin dashed red lines give the ± 1 and ± 2 standard deviation ($\sigma_{\mathrm{experiment}}$) variations in the case of the expected limits, coming from the experimental uncertainties. The maximum sensitivity is reached for the highest Δm ($\Delta m \approx m(\mathrm{W})$), where top squark masses up to 700 GeV are excluded. At the lowest Δm value of 10 GeV covered by the search, the corresponding value is 480 GeV. The reduced sensitivity at lower Δm is explained by the lower transverse momentum spectrum of the decay products, as shown in figure 2, which results in a loss of acceptance.

The limits of the previous analysis are improved. At low Δm the top squark mass limit is 60 GeV higher, thus improving the sensitivity at low mass splittings beyond simple luminosity scaling, while at high Δm the top squark mass limit is extended by 140 GeV. Compared to the results of a similar analysis by the ATLAS Collaboration for the same

JHEP06(2023)060

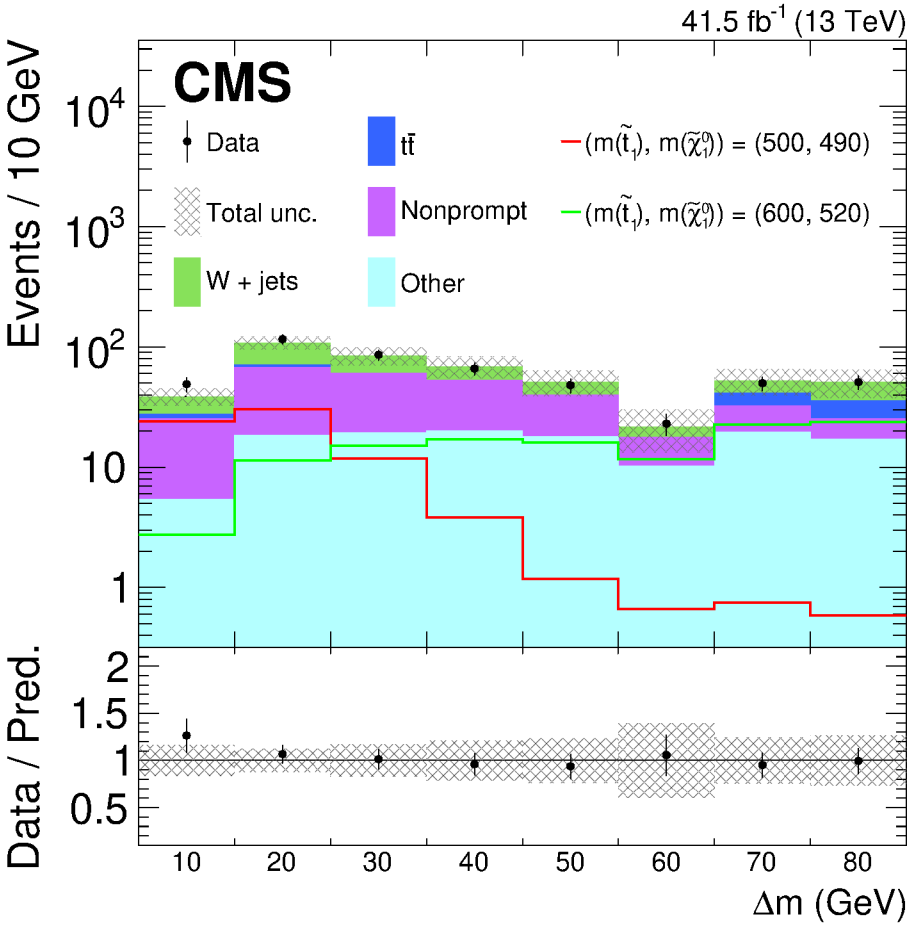

Figure 8. The observed yields in data (points) and the predicted background components (colored histograms) in the eight SRs for the 2017 data. The vertical bars on the points give the statistical uncertainty in the data. The hatched area shows the total uncertainty in the sum of the backgrounds. The expected yields for two signal points with $(m(\tilde{t}_1),\ m(\tilde{\chi}^0_1)) = (500,\ 490)$ and $(600,\ 520)$ GeV are also given by the lines, unstacked from the histograms. The lower panel shows the ratio of the number of observed events to the predicted total background. The vertical bars on the points give the statistical uncertainty in the ratio and the hatched area the total uncertainty.

decay mode and final state [20], the search presented here has comparable limits at intermediate and high Δm values. However, at low Δm, the excluded top squark mass is 120 GeV higher than the ATLAS limit. This is attributed to a more inclusive preselection criteria, where b tagging is not used, and where the discrimination between the signal and the dominating W+jets background is done by a multivariate analysis tool, whose performance is further enhanced by a BDT specifically trained for each Δm.

9 Summary

The results of a search for the direct pair production of top squarks in single-lepton final states are presented within a compressed scenario where R parity is conserved and the mass difference $\Delta m = m(\tilde{t}_1) - m(\tilde{\chi}^0_1)$ between the lightest top squark $(\tilde{t}_1)$ and the lightest

JHEP06(2023)060

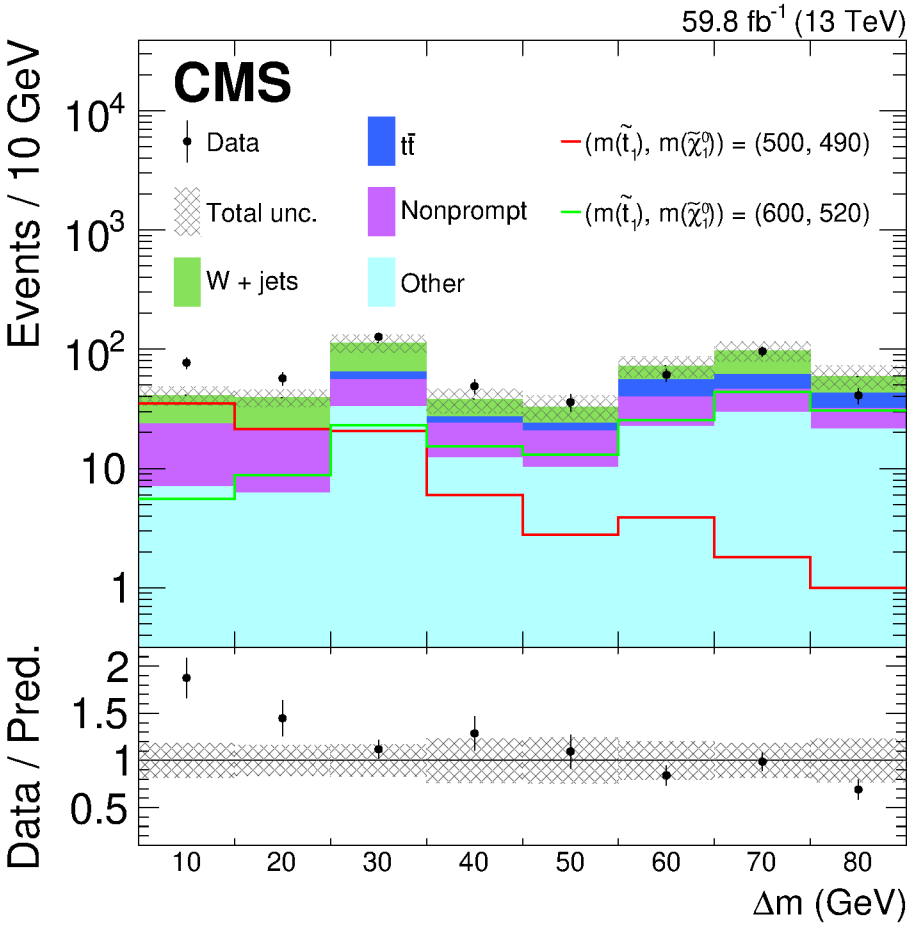

Figure 9. The observed yields in data (points) and the predicted background components (colored histograms) in the eight SRs for the 2018 data. The vertical bars on the points give the statistical uncertainty in the data. The hatched area shows the total uncertainty in the sum of the backgrounds. The expected yields for two signal points with $(m(\tilde{t}_1),\ m(\tilde{\chi}_1^0)) = (500,\ 490)$ and $(600,\ 520)$ GeV are also given by the lines, unstacked from the histograms. The lower panel shows the ratio of the number of observed events to the predicted total background. The vertical bars on the points give the statistical uncertainty in the ratio and the hatched area the total uncertainty.

supersymmetric particle, taken to be the lightest neutralino $\tilde{\chi}_1^0$, does not exceed the W boson mass. The considered decay mode of the top squark is the prompt four-body decay to $\mathrm{bf\bar{f}'}\tilde{\chi}_1^0$, where the fermions in the final state f and $\bar{\mathrm{f}}'$ represent a charged lepton and its neutrino for the decay products of one $\tilde{\mathrm{t}}_1$, and two quarks for the other top squark. The search is based on data collected from proton-proton collisions at $\sqrt{s} = 13\,\mathrm{TeV}$, recorded with the CMS detector during the years 2016, 2017, and 2018, corresponding to an integrated luminosity of $138\,\mathrm{fb}^{-1}$. Events are selected containing a single lepton (electron or muon), at least one high-momentum jet, and significant missing transverse momentum. The analysis is based on a multivariate tool specifically trained for different Δm regions, thus adapting the signal selection to the evolution of the kinematical variables as a function

JHEP06(2023)060

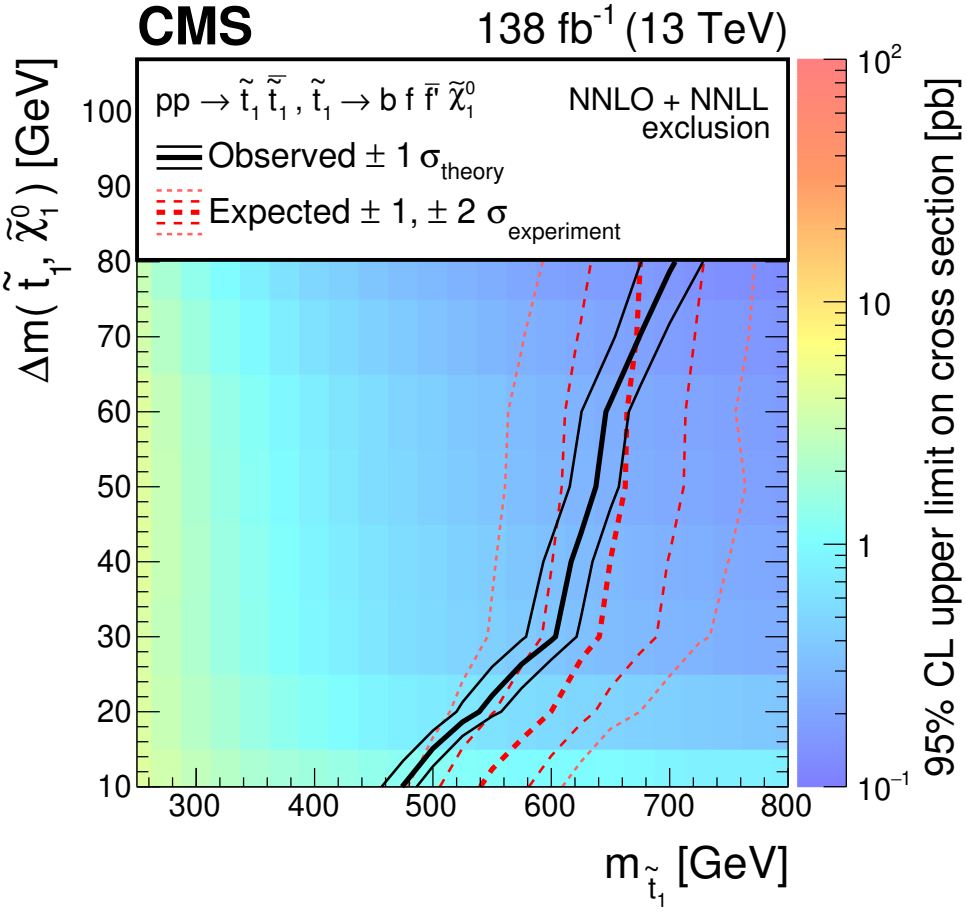

Figure 10. The 95% CL upper limits in the (m($\widetilde{\mathrm{t}}_1$), Δm) plane on the cross section for the production and four-body decay of the top squark using the combined 2016, 2017, and 2018 data. The color shading represents the observed upper limit for a given point in the plane, using the color scale to the right of the figure. The solid black and dashed red lines show the observed and expected 95% CL lower limits, respectively, on m($\widetilde{\mathrm{t}}_1$) as a function of Δm. The thick lines give the central values of the limits. The corresponding thin lines represent the ± 1 standard deviation (σ_{theory}) variations in the limits due to the theoretical uncertainties in the case of the observed limits, and ± 1 and 2 standard deviation ($\sigma_{\mathrm{experiment}}$) variations due to the experimental uncertainties in the case of the expected limits.

of ($m(\widetilde{\mathrm{t}}_1)$, $m(\widetilde{\chi}^0_1)$). The dominant background processes are W+jets, $\mathrm{t\bar{t}}$, and events with nonprompt leptons, which are estimated using control regions in the data.

The observed number of events is consistent with the predicted standard model backgrounds in all signal regions. Upper limits are set at the 95% confidence level on the $\widetilde{\mathrm{t}}_1\bar{\widetilde{\mathrm{t}}}_1$ production cross section as a function of the $\widetilde{\mathrm{t}}_1$ and $\widetilde{\chi}^0_1$ masses, within the context of a simplified model. Assuming a 100% branching fraction in the four-body decay mode, the search excludes top squark masses up to 480 and 700 GeV at $\Delta m = 10$ and 80 GeV, respectively. The results summarized in this paper are among the best limits to date on the top squark pair production cross section, where the top squark decays via the four-body mode, and currently correspond to the most stringent limits for $\Delta m < 30$ GeV.

JHEP06(2023)060

Acknowledgments

We congratulate our colleagues in the CERN accelerator departments for the excellent performance of the LHC and thank the technical and administrative staffs at CERN and at other CMS institutes for their contributions to the success of the CMS effort. In addition, we gratefully acknowledge the computing centers and personnel of the Worldwide LHC Computing Grid and other centers for delivering so effectively the computing infrastructure essential to our analyses. Finally, we acknowledge the enduring support for the construction and operation of the LHC, the CMS detector, and the supporting computing infrastructure provided by the following funding agencies: BMBWF and FWF (Austria); FNRS and FWO (Belgium); CNPq, CAPES, FAPERJ, FAPERGS, and FAPESP (Brazil); MES and BNSF (Bulgaria); CERN; CAS, MoST, and NSFC (China); MINCIENCIAS (Colombia); MSES and CSF (Croatia); RIF (Cyprus); SENESCYT (Ecuador); MoER, ERC PUT and ERDF (Estonia); Academy of Finland, MEC, and HIP (Finland); CEA and CNRS/IN2P3 (France); BMBF, DFG, and HGF (Germany); GSRI (Greece); NKFIH (Hungary); DAE and DST (India); IPM (Iran); SFI (Ireland); INFN (Italy); MSIP and NRF (Republic of Korea); MES (Latvia); LAS (Lithuania); MOE and UM (Malaysia); BUAP, CINVESTAV, CONACYT, LNS, SEP, and UASLP-FAI (Mexico); MOS (Montenegro); MBIE (New Zealand); PAEC (Pakistan); MES and NSC (Poland); FCT (Portugal); MESTD (Serbia); MCIN/AEI and PCTI (Spain); MOSTR (Sri Lanka); Swiss Funding Agencies (Switzerland); MST (Taipei); MHESI and NSTDA (Thailand); TUBITAK and TENMAK (Turkey); NASU (Ukraine); STFC (United Kingdom); DOE and NSF (U.S.A.).

Individuals have received support from the Marie-Curie program and the European Research Council and Horizon 2020 Grant, contract Nos. 675440, 724704, 752730, 758316, 765710, 824093, 884104, and COST Action CA16108 (European Union); the Leventis Foundation; the Alfred P. Sloan Foundation; the Alexander von Humboldt Foundation; the Belgian Federal Science Policy Office; the Fonds pour la Formation à la Recherche dans l'Industrie et dans l'Agriculture (FRIA-Belgium); the Agentschap voor Innovatie door Wetenschap en Technologie (IWT-Belgium); the F.R.S.-FNRS and FWO (Belgium) under the "Excellence of Science — EOS" — be.h project n. 30820817; the Beijing Municipal Science & Technology Commission, No. Z191100007219010; the Ministry of Education, Youth and Sports (MEYS) of the Czech Republic; the Hellenic Foundation for Research and Innovation (HFRI), Project Number 2288 (Greece); the Deutsche Forschungsgemeinschaft (DFG), under Germany's Excellence Strategy — EXC 2121 "Quantum Universe" — 390833306, and under project number 400140256 - GRK2497; the Hungarian Academy of Sciences, the New National Excellence Program - ÚNKP, the NKFIH research grants K 124845, K 124850, K 128713, K 128786, K 129058, K 131991, K 133046, K 138136, K 143460, K 143477, 2020-2.2.1-ED-2021-00181, and TKP2021-NKTA-64 (Hungary); the Council of Science and Industrial Research, India; the Latvian Council of Science; the Ministry of Education and Science, project no. 2022/WK/14, and the National Science Center, contracts Opus 2021/41/B/ST2/01369 and 2021/43/B/ST2/01552 (Poland); the Fundação para a Ciência e a Tecnologia, grant CEECIND/01334/2018 (Portugal); MCIN/AEI/10.13039/501100011033, ERDF "a way of making Europe", and the Programa

JHEP06(2023)060

Estatal de Fomento de la Investigación Científica y Técnica de Excelencia María de Maeztu, grant MDM-2017-0765 and Programa Severo Ochoa del Principado de Asturias (Spain); the Chulalongkorn Academic into Its 2nd Century Project Advancement Project, and the National Science, Research and Innovation Fund via the Program Management Unit for Human Resources & Institutional Development, Research and Innovation, grant B05F650021 (Thailand); the Kavli Foundation; the Nvidia Corporation; the SuperMicro Corporation; the Welch Foundation, contract C-1845; and the Weston Havens Foundation (U.S.A.).

JHEP06(2023)060

References

[1] S.P. Martin, *A supersymmetry primer*, *Adv. Ser. Direct. High Energy Phys.* **18** (1998) 1 [hep-ph/9709356] [INSPIRE].

[2] J. Wess and B. Zumino, *Supergauge transformations in four-dimensions*, *Nucl. Phys. B* **70** (1974) 39 [INSPIRE].

[3] H.P. Nilles, *Supersymmetry, supergravity and particle physics*, *Phys. Rept.* **110** (1984) 1 [INSPIRE].

[4] H.E. Haber and G.L. Kane, *The search for supersymmetry: probing physics beyond the standard model*, *Phys. Rept.* **117** (1985) 75 [INSPIRE].

[5] R. Barbieri, S. Ferrara and C.A. Savoy, *Gauge models with spontaneously broken local supersymmetry*, *Phys. Lett. B* **119** (1982) 343 [INSPIRE].

[6] S. Dawson, E. Eichten and C. Quigg, *Search for supersymmetric particles in hadron-hadron collisions*, *Phys. Rev. D* **31** (1985) 1581 [INSPIRE].

[7] ATLAS collaboration, *Observation of a new particle in the search for the standard model Higgs boson with the ATLAS detector at the LHC*, *Phys. Lett. B* **716** (2012) 1 [arXiv:1207.7214] [INSPIRE].

[8] CMS collaboration, *Observation of a new boson at a mass of* 125 *GeV with the CMS experiment at the LHC*, *Phys. Lett. B* **716** (2012) 30 [arXiv:1207.7235] [INSPIRE].

[9] CMS collaboration, *Observation of a new boson with mass near* 125 *GeV in pp collisions at* $\sqrt{s} = 7$ *and* 8 *TeV*, *JHEP* **06** (2013) 081 [arXiv:1303.4571] [INSPIRE].

[10] G.R. Farrar and P. Fayet, *Phenomenology of the production, decay, and detection of new hadronic states associated with supersymmetry*, *Phys. Lett. B* **76** (1978) 575 [INSPIRE].

[11] C. Balázs, M. Carena and C.E.M. Wagner, *Dark matter, light stops and electroweak baryogenesis*, *Phys. Rev. D* **70** (2004) 015007 [hep-ph/0403224] [INSPIRE].

[12] T. Cohen et al., *SUSY simplified models at* 14, 33, *and* 100 *TeV proton colliders*, *JHEP* **04** (2014) 117 [arXiv:1311.6480] [INSPIRE].

[13] N. Arkani-Hamed et al., *MARMOSET: the path from LHC data to the new standard model via on-shell effective theories*, hep-ph/0703088 [INSPIRE].

[14] J. Alwall, P. Schuster and N. Toro, *Simplified models for a first characterization of new physics at the LHC*, *Phys. Rev. D* **79** (2009) 075020 [arXiv:0810.3921] [INSPIRE].

[15] J. Alwall, M.-P. Le, M. Lisanti and J.G. Wacker, *Model-independent jets plus missing energy searches*, *Phys. Rev. D* **79** (2009) 015005 [arXiv:0809.3264] [INSPIRE].

[16] LHC New Physics Working Group collaboration, *Simplified models for LHC new physics searches*, *J. Phys. G* **39** (2012) 105005 [arXiv:1105.2838] [INSPIRE].

[17] CMS collaboration, *Interpretation of searches for supersymmetry with simplified models*, *Phys. Rev. D* **88** (2013) 052017 [arXiv:1301.2175] [INSPIRE].

[18] CMS collaboration, *Search for top squarks decaying via four-body or chargino-mediated modes in single-lepton final states in proton-proton collisions at* $\sqrt{s} = 13$ *TeV*, *JHEP* **09** (2018) 065 [arXiv:1805.05784] [INSPIRE].

[19] CMS collaboration, *Precision luminosity measurement in proton-proton collisions at* $\sqrt{s} = 13$ *TeV in* 2015 *and* 2016 *at CMS*, *Eur. Phys. J. C* **81** (2021) 800 [arXiv:2104.01927] [INSPIRE].

[20] ATLAS collaboration, *Search for new phenomena with top quark pairs in final states with one lepton, jets, and missing transverse momentum in pp collisions at* $\sqrt{s} = 13$ *TeV with the ATLAS detector*, *JHEP* **04** (2021) 174 [arXiv:2012.03799] [INSPIRE].

[21] *HEPData record for this analysis*, (2022) [DOI:10.17182/hepdata.135455].

[22] CMS collaboration, *The CMS experiment at the CERN LHC*, 2008 *JINST* **3** S08004 [INSPIRE].

[23] CMS collaboration, *Performance of the CMS level-1 trigger in proton-proton collisions at* $\sqrt{s} = 13$ *TeV*, 2020 *JINST* **15** P10017 [arXiv:2006.10165] [INSPIRE].

[24] CMS collaboration, *The CMS trigger system*, 2017 *JINST* **12** P01020 [arXiv:1609.02366] [INSPIRE].

[25] CMS collaboration, *Electron and photon reconstruction and identification with the CMS experiment at the CERN LHC*, 2021 *JINST* **16** P05014 [arXiv:2012.06888] [INSPIRE].

[26] CMS collaboration, *Performance of the CMS muon detector and muon reconstruction with proton-proton collisions at* $\sqrt{s} = 13$ *TeV*, 2018 *JINST* **13** P06015 [arXiv:1804.04528] [INSPIRE].

[27] CMS collaboration, *Description and performance of track and primary-vertex reconstruction with the CMS tracker*, 2014 *JINST* **9** P10009 [arXiv:1405.6569] [INSPIRE].

[28] J. Alwall et al., *The automated computation of tree-level and next-to-leading order differential cross sections, and their matching to parton shower simulations*, *JHEP* **07** (2014) 079 [arXiv:1405.0301] [INSPIRE].

[29] P. Nason, *A new method for combining NLO QCD with shower Monte Carlo algorithms*, *JHEP* **11** (2004) 040 [hep-ph/0409146] [INSPIRE].

[30] S. Frixione, P. Nason and C. Oleari, *Matching NLO QCD computations with parton shower simulations: the POWHEG method*, *JHEP* **11** (2007) 070 [arXiv:0709.2092] [INSPIRE].

[31] S. Alioli, P. Nason, C. Oleari and E. Re, *A general framework for implementing NLO calculations in shower Monte Carlo programs: the POWHEG BOX*, *JHEP* **06** (2010) 043 [arXiv:1002.2581] [INSPIRE].

JHEP06(2023)060

[32] S. Alioli, P. Nason, C. Oleari and E. Re, *NLO single-top production matched with shower in POWHEG: s- and t-channel contributions*, *JHEP* **09** (2009) 111 [*Erratum ibid.* **02** (2010) 011] [arXiv:0907.4076] [INSPIRE].

[33] E. Re, *Single-top Wt-channel production matched with parton showers using the POWHEG method*, *Eur. Phys. J. C* **71** (2011) 1547 [arXiv:1009.2450] [INSPIRE].

[34] T. Melia, P. Nason, R. Röntsch and G. Zanderighi, W^+W^-, WZ *and* ZZ *production in the POWHEG BOX*, *JHEP* **11** (2011) 078 [arXiv:1107.5051] [INSPIRE].

[35] P. Nason and G. Zanderighi, W^+W^-, WZ *and* ZZ *production in the POWHEG-BOX-V2*, *Eur. Phys. J. C* **74** (2014) 2702 [arXiv:1311.1365] [INSPIRE].

[36] H.B. Hartanto, B. Jäger, L. Reina and D. Wackeroth, *Higgs boson production in association with top quarks in the POWHEG BOX*, *Phys. Rev. D* **91** (2015) 094003 [arXiv:1501.04498] [INSPIRE].

[37] NNPDF collaboration, *Parton distributions from high-precision collider data*, *Eur. Phys. J. C* **77** (2017) 663 [arXiv:1706.00428] [INSPIRE].

[38] R. Frederix and S. Frixione, *Merging meets matching in MC@NLO*, *JHEP* **12** (2012) 061 [arXiv:1209.6215] [INSPIRE].

[39] T. Sjöstrand et al., *An introduction to PYTHIA* 8.2, *Comput. Phys. Commun.* **191** (2015) 159 [arXiv:1410.3012] [INSPIRE].

[40] CMS collaboration, *Extraction and validation of a new set of CMS PYTHIA*8 *tunes from underlying-event measurements*, *Eur. Phys. J. C* **80** (2020) 4 [arXiv:1903.12179] [INSPIRE].

[41] GEANT4 collaboration, *GEANT*4 — *a simulation toolkit*, *Nucl. Instrum. Meth. A* **506** (2003) 250 [INSPIRE].

[42] W. Beenakker, R. Höpker and M. Spira, *PROSPINO: a program for the production of supersymmetric particles in next-to-leading order QCD*, hep-ph/9611232.

[43] C. Borschensky et al., *Squark and gluino production cross sections in pp collisions at* $\sqrt{s} = 13$, 14, 33 *and* 100 *TeV*, *Eur. Phys. J. C* **74** (2014) 3174 [arXiv:1407.5066] [INSPIRE].

[44] W. Beenakker, R. Höpker, M. Spira and P.M. Zerwas, *Squark and gluino production at hadron colliders*, *Nucl. Phys. B* **492** (1997) 51 [hep-ph/9610490] [INSPIRE].

[45] A. Kulesza and L. Motyka, *Threshold resummation for squark-antisquark and gluino-pair production at the LHC*, *Phys. Rev. Lett.* **102** (2009) 111802 [arXiv:0807.2405] [INSPIRE].

[46] A. Kulesza and L. Motyka, *Soft gluon resummation for the production of gluino-gluino and squark-antisquark pairs at the LHC*, *Phys. Rev. D* **80** (2009) 095004 [arXiv:0905.4749] [INSPIRE].

[47] W. Beenakker et al., *Soft-gluon resummation for squark and gluino hadroproduction*, *JHEP* **12** (2009) 041 [arXiv:0909.4418] [INSPIRE].

[48] W. Beenakker et al., *Squark and gluino hadroproduction*, *Int. J. Mod. Phys. A* **26** (2011) 2637 [arXiv:1105.1110] [INSPIRE].

[49] W. Beenakker et al., *NNLL-fast: predictions for coloured supersymmetric particle production at the LHC with threshold and Coulomb resummation*, *JHEP* **12** (2016) 133 [arXiv:1607.07741] [INSPIRE].

[50] W. Beenakker et al., *NNLL resummation for stop pair-production at the LHC*, *JHEP* **05** (2016) 153 [arXiv:1601.02954] [INSPIRE].

JHEP06(2023)060

[51] CMS collaboration, *The fast simulation of the CMS detector at LHC*, *J. Phys. Conf. Ser.* **331** (2011) 032049 [INSPIRE].

[52] A. Giammanco, *The fast simulation of the CMS experiment*, *J. Phys. Conf. Ser.* **513** (2014) 022012 [INSPIRE].

[53] CMS collaboration, *Particle-flow reconstruction and global event description with the CMS detector*, 2017 *JINST* **12** P10003 [arXiv:1706.04965] [INSPIRE].

[54] D. Contardo et al., *Technical proposal for the phase-II upgrade of the CMS detector*, CERN-LHCC-2015-010, CERN, Geneva, Switzerland (2015) [DOI:10.17181/CERN.VU8I.D59J].

[55] M. Cacciari, G.P. Salam and G. Soyez, *The anti-k_t jet clustering algorithm*, *JHEP* **04** (2008) 063 [arXiv:0802.1189] [INSPIRE].

[56] M. Cacciari, G.P. Salam and G. Soyez, *FastJet user manual*, *Eur. Phys. J. C* **72** (2012) 1896 [arXiv:1111.6097] [INSPIRE].

[57] CMS collaboration, *Jet energy scale and resolution in the CMS experiment in pp collisions at 8 TeV*, 2017 *JINST* **12** P02014 [arXiv:1607.03663] [INSPIRE].

[58] CMS collaboration, *Identification of heavy-flavour jets with the CMS detector in pp collisions at 13 TeV*, 2018 *JINST* **13** P05011 [arXiv:1712.07158] [INSPIRE].

[59] CMS collaboration, *Performance of the DeepJet b tagging algorithm using 41.9 fb^{-1} of data from proton-proton collisions at 13 TeV with phase 1 CMS detector*, CMS-DP-2018-058, CERN, Geneva, Switzerland (2018).

[60] CMS collaboration, *Performance of missing transverse momentum reconstruction in proton-proton collisions at $\sqrt{s} = 13$ TeV using the CMS detector*, 2019 *JINST* **14** P07004 [arXiv:1903.06078] [INSPIRE].

[61] CMS collaboration, *Search for supersymmetry in pp collisions at $\sqrt{s} = 13$ TeV in the single-lepton final state using the sum of masses of large-radius jets*, *JHEP* **08** (2016) 122 [arXiv:1605.04608] [INSPIRE].

[62] K. Rehermann and B. Tweedie, *Efficient identification of boosted semileptonic top quarks at the LHC*, *JHEP* **03** (2011) 059 [arXiv:1007.2221] [INSPIRE].

[63] L. Rokach and O. Maimon, *Data mining with decision trees: theory and applications*, World Scientific (2008).

[64] A. Hocker et al., *TMVA — toolkit for multivariate data analysis*, *PoS* **ACAT** (2007) 040 [physics/0703039] [INSPIRE].

[65] G. Cowan, K. Cranmer, E. Gross and O. Vitells, *Asymptotic formulae for likelihood-based tests of new physics*, *Eur. Phys. J. C* **71** (2011) 1554 [*Erratum ibid.* **73** (2013) 2501] [arXiv:1007.1727] [INSPIRE].

[66] CMS collaboration, *Search for new physics in same-sign dilepton events in proton-proton collisions at $\sqrt{s} = 13$ TeV*, *Eur. Phys. J. C* **76** (2016) 439 [arXiv:1605.03171] [INSPIRE].

[67] CMS collaboration, *CMS luminosity measurement for the 2017 data-taking period at $\sqrt{s} = 13$ TeV*, CMS-PAS-LUM-17-004, CERN, Geneva, Switzerland (2018).

[68] CMS collaboration, *CMS luminosity measurement for the 2018 data-taking period at $\sqrt{s} = 13$ TeV*, CMS-PAS-LUM-18-002, CERN, Geneva, Switzerland (2019).

[69] CMS collaboration, *Measurement of the inelastic proton-proton cross section at $\sqrt{s} = 13$ TeV*, *JHEP* **07** (2018) 161 [arXiv:1802.02613] [INSPIRE].

JHEP06(2023)060

[70] A. Kalogeropoulos and J. Alwall, *The SysCalc code: a tool to derive theoretical systematic uncertainties*, arXiv:1801.08401 [INSPIRE].

[71] T. Junk, *Confidence level computation for combining searches with small statistics*, *Nucl. Instrum. Meth. A* **434** (1999) 435 [hep-ex/9902006] [INSPIRE].

[72] A.L. Read, *Presentation of search results: the CL_s technique*, *J. Phys. G* **28** (2002) 2693 [INSPIRE].

[73] ATLAS collaboration, *Primary vertex identification using deep learning in ATLAS*, ATL-PHYS-PUB-2023-011, CERN, Geneva, Switzerland (2023).

JHEP06(2023)060

The CMS collaboration

Yerevan Physics Institute, Yerevan, Armenia

A. Tumasyan

Institut für Hochenergiephysik, Vienna, Austria

W. Adam, J.W. Andrejkovic, T. Bergauer, S. Chatterjee, K. Damanakis, M. Dragicevic, A. Escalante Del Valle, P.S. Hussain, M. Jeitler[1], N. Krammer, L. Lechner, D. Liko, I. Mikulec, P. Paulitsch, F.M. Pitters, J. Schieck[1], R. Schöfbeck, D. Schwarz, M. Sonawane, S. Templ, W. Waltenberger, C.-E. Wulz[1]

Universiteit Antwerpen, Antwerpen, Belgium

M.R. Darwish[2], T. Janssen, T. Kello[3], H. Rejeb Sfar, P. Van Mechelen

Vrije Universiteit Brussel, Brussel, Belgium

E.S. Bols, J. D'Hondt, A. De Moor, M. Delcourt, H. El Faham, S. Lowette, S. Moortgat, A. Morton, D. Müller, A.R. Sahasransu, S. Tavernier, W. Van Doninck, D. Vannerom

Université Libre de Bruxelles, Bruxelles, Belgium

B. Clerbaux, G. De Lentdecker, L. Favart, D. Hohov, J. Jaramillo, K. Lee, M. Mahdavikhorrami, I. Makarenko, A. Malara, S. Paredes, L. Pétré, N. Postiau, L. Thomas, M. Vanden Bemden, C. Vander Velde, P. Vanlaer

Ghent University, Ghent, Belgium

D. Dobur, J. Knolle, L. Lambrecht, G. Mestdach, C. Rendón, A. Samalan, K. Skovpen, M. Tytgat, N. Van Den Bossche, B. Vermassen, L. Wezenbeek

Université Catholique de Louvain, Louvain-la-Neuve, Belgium

A. Benecke, G. Bruno, F. Bury, C. Caputo, P. David, C. Delaere, I.S. Donertas, A. Giammanco, K. Jaffel, Sa. Jain, V. Lemaitre, K. Mondal, A. Taliercio, T.T. Tran, P. Vischia, S. Wertz

Centro Brasileiro de Pesquisas Fisicas, Rio de Janeiro, Brazil

G.A. Alves, E. Coelho, C. Hensel, A. Moraes, P. Rebello Teles

Universidade do Estado do Rio de Janeiro, Rio de Janeiro, Brazil

W.L. Aldá Júnior, M. Alves Gallo Pereira, M. Barroso Ferreira Filho, H. Brandao Malbouisson, W. Carvalho, J. Chinellato[4], E.M. Da Costa, G.G. Da Silveira[5], D. De Jesus Damiao, V. Dos Santos Sousa, S. Fonseca De Souza, J. Martins[6], C. Mora Herrera, K. Mota Amarilo, L. Mundim, H. Nogima, A. Santoro, S.M. Silva Do Amaral, A. Sznajder, M. Thiel, A. Vilela Pereira

JHEP06(2023)060

Universidade Estadual Paulista, Universidade Federal do ABC, São Paulo, Brazil

C.A. Bernardes[5], L. Calligaris, T.R. Fernandez Perez Tomei, E.M. Gregores, P.G. Mercadante, S.F. Novaes, Sandra S. Padula

Institute for Nuclear Research and Nuclear Energy, Bulgarian Academy of Sciences, Sofia, Bulgaria

A. Aleksandrov, G. Antchev, R. Hadjiiska, P. Iaydjiev, M. Misheva, M. Rodozov, M. Shopova, G. Sultanov

University of Sofia, Sofia, Bulgaria

A. Dimitrov, T. Ivanov, L. Litov, B. Pavlov, P. Petkov, A. Petrov, E. Shumka

Instituto De Alta Investigación, Universidad de Tarapacá, Casilla 7 D, Arica, Chile

S.Thakur

Beihang University, Beijing, China

T. Cheng, T. Javaid[7], M. Mittal, L. Yuan

Department of Physics, Tsinghua University, Beijing, China

M. Ahmad, G. Bauer[8], Z. Hu, S. Lezki, K. Yi[8,9]

Institute of High Energy Physics, Beijing, China

G.M. Chen[7], H.S. Chen[7], M. Chen[7], F. Iemmi, C.H. Jiang, A. Kapoor, H. Liao, Z.-A. Liu[10], V. Milosevic, F. Monti, R. Sharma, J. Tao, J. Thomas-Wilsker, J. Wang, H. Zhang, J. Zhao

State Key Laboratory of Nuclear Physics and Technology, Peking University, Beijing, China

A. Agapitos, Y. An, Y. Ban, A. Levin, C. Li, Q. Li, X. Lyu, Y. Mao, S.J. Qian, X. Sun, D. Wang, J. Xiao, H. Yang

Sun Yat-Sen University, Guangzhou, China

M. Lu, Z. You

University of Science and Technology of China, Hefei, China

N. Lu

Institute of Modern Physics and Key Laboratory of Nuclear Physics and Ion-beam Application (MOE) - Fudan University, Shanghai, China

X. Gao[3], D. Leggat, H. Okawa, Y. Zhang

Zhejiang University, Hangzhou, Zhejiang, China

Z. Lin, C. Lu, M. Xiao

JHEP06(2023)060

Universidad de Los Andes, Bogota, Colombia
C. Avila, D.A. Barbosa Trujillo, A. Cabrera, C. Florez, J. Fraga

Universidad de Antioquia, Medellin, Colombia
J. Mejia Guisao, F. Ramirez, M. Rodriguez, J.D. Ruiz Alvarez

University of Split, Faculty of Electrical Engineering, Mechanical Engineering and Naval Architecture, Split, Croatia
D. Giljanovic, N. Godinovic, D. Lelas, I. Puljak

University of Split, Faculty of Science, Split, Croatia
Z. Antunovic, M. Kovac, T. Sculac

Institute Rudjer Boskovic, Zagreb, Croatia
V. Brigljevic, B.K. Chitroda, D. Ferencek, S. Mishra, M. Roguljic, A. Starodumov[11], T. Susa

University of Cyprus, Nicosia, Cyprus
A. Attikis, K. Christoforou, M. Kolosova, S. Konstantinou, J. Mousa, C. Nicolaou, F. Ptochos, P.A. Razis, H. Rykaczewski, H. Saka, A. Stepennov

Charles University, Prague, Czech Republic
M. Finger[11], M. Finger Jr.[11], A. Kveton

Escuela Politecnica Nacional, Quito, Ecuador
E. Ayala

Universidad San Francisco de Quito, Quito, Ecuador
E. Carrera Jarrin

Academy of Scientific Research and Technology of the Arab Republic of Egypt, Egyptian Network of High Energy Physics, Cairo, Egypt
H. Abdalla[12], Y. Assran[13,14]

Center for High Energy Physics (CHEP-FU), Fayoum University, El-Fayoum, Egypt
M.A. Mahmoud, Y. Mohammed

National Institute of Chemical Physics and Biophysics, Tallinn, Estonia
S. Bhowmik, R.K. Dewanjee, K. Ehataht, M. Kadastik, T. Lange, S. Nandan, C. Nielsen, J. Pata, M. Raidal, L. Tani, C. Veelken

Department of Physics, University of Helsinki, Helsinki, Finland
P. Eerola, H. Kirschenmann, K. Osterberg, M. Voutilainen

JHEP06(2023)060

Helsinki Institute of Physics, Helsinki, Finland
S. Bharthuar, E. Brücken, F. Garcia, J. Havukainen, M.S. Kim, R. Kinnunen, T. Lampén, K. Lassila-Perini, S. Lehti, T. Lindén, M. Lotti, L. Martikainen, M. Myllymäki, J. Ott, M.m. Rantanen, H. Siikonen, E. Tuominen, J. Tuominiemi

Lappeenranta-Lahti University of Technology, Lappeenranta, Finland
P. Luukka, H. Petrow, T. Tuuva

IRFU, CEA, Université Paris-Saclay, Gif-sur-Yvette, France
C. Amendola, M. Besancon, F. Couderc, M. Dejardin, D. Denegri, J.L. Faure, F. Ferri, S. Ganjour, P. Gras, G. Hamel de Monchenault, V. Lohezic, J. Malcles, J. Rander, A. Rosowsky, M.Ö. Sahin, A. Savoy-Navarro[15], P. Simkina, M. Titov

Laboratoire Leprince-Ringuet, CNRS/IN2P3, Ecole Polytechnique, Institut Polytechnique de Paris, Palaiseau, France
C. Baldenegro Barrera, F. Beaudette, A. Buchot Perraguin, P. Busson, A. Cappati, C. Charlot, F. Damas, O. Davignon, B. Diab, G. Falmagne, B.A. Fontana Santos Alves, S. Ghosh, R. Granier de Cassagnac, A. Hakimi, B. Harikrishnan, G. Liu, J. Motta, M. Nguyen, C. Ochando, L. Portales, R. Salerno, U. Sarkar, J.B. Sauvan, Y. Sirois, A. Tarabini, E. Vernazza, A. Zabi, A. Zghiche

Université de Strasbourg, CNRS, IPHC UMR 7178, Strasbourg, France
J.-L. Agram[16], J. Andrea, D. Apparu, D. Bloch, G. Bourgatte, J.-M. Brom, E.C. Chabert, C. Collard, D. Darej, U. Goerlach, C. Grimault, A.-C. Le Bihan, P. Van Hove

Institut de Physique des 2 Infinis de Lyon (IP2I), Villeurbanne, France
S. Beauceron, B. Blancon, G. Boudoul, A. Carle, N. Chanon, J. Choi, D. Contardo, P. Depasse, C. Dozen[17], H. El Mamouni, J. Fay, S. Gascon, M. Gouzevitch, G. Grenier, B. Ille, I.B. Laktineh, M. Lethuillier, L. Mirabito, S. Perries, L. Torterotot, M. Vander Donckt, P. Verdier, S. Viret

Georgian Technical University, Tbilisi, Georgia
A. Khvedelidze[11], I. Lomidze, Z. Tsamalaidze[11]

RWTH Aachen University, I. Physikalisches Institut, Aachen, Germany
V. Botta, L. Feld, K. Klein, M. Lipinski, D. Meuser, A. Pauls, N. Röwert, M. Teroerde

RWTH Aachen University, III. Physikalisches Institut A, Aachen, Germany
S. Diekmann, A. Dodonova, N. Eich, D. Eliseev, M. Erdmann, P. Fackeldey, D. Fasanella, B. Fischer, T. Hebbeker, K. Hoepfner, F. Ivone, M.y. Lee, L. Mastrolorenzo, M. Merschmeyer, A. Meyer, S. Mondal, S. Mukherjee, D. Noll, A. Novak, F. Nowotny, A. Pozdnyakov, Y. Rath, W. Redjeb, H. Reithler, A. Schmidt,

JHEP06(2023)060

S.C. Schuler, A. Sharma, A. Stein, F. Torres Da Silva De Araujo[18], L. Vigilante, S. Wiedenbeck, S. Zaleski

RWTH Aachen University, III. Physikalisches Institut B, Aachen, Germany

C. Dziwok, G. Flügge, W. Haj Ahmad[19], O. Hlushchenko, T. Kress, A. Nowack, O. Pooth, A. Stahl, T. Ziemons, A. Zotz

Deutsches Elektronen-Synchrotron, Hamburg, Germany

H. Aarup Petersen, M. Aldaya Martin, P. Asmuss, S. Baxter, M. Bayatmakou, O. Behnke, A. Bermúdez Martínez, S. Bhattacharya, A.A. Bin Anuar, F. Blekman[20], K. Borras[21], D. Brunner, A. Campbell, A. Cardini, C. Cheng, F. Colombina, S. Consuegra Rodríguez, G. Correia Silva, M. De Silva, L. Didukh, G. Eckerlin, D. Eckstein, L.I. Estevez Banos, O. Filatov, E. Gallo[20], A. Geiser, A. Giraldi, G. Greau, A. Grohsjean, V. Guglielmi, M. Guthoff, A. Jafari[22], N.Z. Jomhari, B. Kaech, M. Kasemann, H. Kaveh, C. Kleinwort, R. Kogler, M. Komm, D. Krücker, W. Lange, D. Leyva Pernia, K. Lipka[23], W. Lohmann[24], R. Mankel, I.-A. Melzer-Pellmann, M. Mendizabal Morentin, J. Metwally, A.B. Meyer, G. Milella, M. Mormile, A. Mussgiller, A. Nürnberg, Y. Otarid, D. Pérez Adán, A. Raspereza, B. Ribeiro Lopes, J. Rübenach, A. Saggio, A. Saibel, M. Savitskyi, M. Scham[25,21], V. Scheurer, S. Schnake[21], P. Schütze, C. Schwanenberger[20], M. Shchedrolosiev, R.E. Sosa Ricardo, D. Stafford, N. Tonon[†], M. Van De Klundert, F. Vazzoler, A. Velyka, A. Ventura Barroso, R. Walsh, D. Walter, Q. Wang, Y. Wen, K. Wichmann, L. Wiens[21], C. Wissing, S. Wuchterl, Y. Yang, A. Zimermmane Castro Santos

University of Hamburg, Hamburg, Germany

A. Albrecht, S. Albrecht, M. Antonello, S. Bein, L. Benato, M. Bonanomi, P. Connor, K. De Leo, M. Eich, K. El Morabit, F. Feindt, A. Fröhlich, C. Garbers, E. Garutti, M. Hajheidari, J. Haller, A. Hinzmann, H.R. Jabusch, G. Kasieczka, P. Keicher, R. Klanner, W. Korcari, T. Kramer, V. Kutzner, F. Labe, J. Lange, A. Lobanov, C. Matthies, A. Mehta, L. Moureaux, M. Mrowietz, A. Nigamova, Y. Nissan, A. Paasch, K.J. Pena Rodriguez, T. Quadfasel, M. Rieger, O. Rieger, D. Savoiu, J. Schindler, P. Schleper, M. Schröder, J. Schwandt, M. Sommerhalder, H. Stadie, G. Steinbrück, A. Tews, M. Wolf

Karlsruher Institut fuer Technologie, Karlsruhe, Germany

S. Brommer, M. Burkart, E. Butz, R. Caspart, T. Chwalek, A. Dierlamm, A. Droll, N. Faltermann, M. Giffels, J.O. Gosewisch, A. Gottmann, F. Hartmann[26], M. Horzela, U. Husemann, M. Klute, R. Koppenhöfer, M. Link, A. Lintuluoto, S. Maier, S. Mitra, Th. Müller, M. Neukum, M. Oh, G. Quast, K. Rabbertz, J. Rauser, M. Schnepf, I. Shvetsov, H.J. Simonis, N. Trevisani, R. Ulrich, J. van der Linden, R.F. Von Cube, M. Wassmer, S. Wieland, R. Wolf, S. Wozniewski, S. Wunsch, X. Zuo

JHEP06(2023)060

Institute of Nuclear and Particle Physics (INPP), NCSR Demokritos, Aghia Paraskevi, Greece

G. Anagnostou, P. Assiouras, G. Daskalakis, A. Kyriakis, A. Stakia

National and Kapodistrian University of Athens, Athens, Greece

M. Diamantopoulou, D. Karasavvas, P. Kontaxakis, A. Manousakis-Katsikakis, A. Panagiotou, I. Papavergou, N. Saoulidou, K. Theofilatos, E. Tziaferi, K. Vellidis, I. Zisopoulos

National Technical University of Athens, Athens, Greece

G. Bakas, T. Chatzistavrou, K. Kousouris, I. Papakrivopoulos, G. Tsipolitis, A. Zacharopoulou

University of Ioánnina, Ioánnina, Greece

K. Adamidis, I. Bestintzanos, I. Evangelou, C. Foudas, P. Gianneios, C. Kamtsikis, P. Katsoulis, P. Kokkas, P.G. Kosmoglou Kioseoglou, N. Manthos, I. Papadopoulos, J. Strologas

MTA-ELTE Lendület CMS Particle and Nuclear Physics Group, Eötvös Loránd University, Budapest, Hungary

M. Csanád, K. Farkas, M.M.A. Gadallah[27], S. Lökös[28], P. Major, K. Mandal, G. Pásztor, A.J. Rádl[29], O. Surányi, G.I. Veres

Wigner Research Centre for Physics, Budapest, Hungary

M. Bartók[30], G. Bencze, C. Hajdu, D. Horvath[31,32], F. Sikler, V. Veszpremi

Institute of Nuclear Research ATOMKI, Debrecen, Hungary

N. Beni, S. Czellar, J. Karancsi[30], J. Molnar, Z. Szillasi, D. Teyssier

Institute of Physics, University of Debrecen, Debrecen, Hungary

P. Raics, B. Ujvari[33]

Karoly Robert Campus, MATE Institute of Technology, Gyongyos, Hungary

T. Csorgo[29], F. Nemes[29], T. Novak

Panjab University, Chandigarh, India

J. Babbar, S. Bansal, S.B. Beri, V. Bhatnagar, G. Chaudhary, S. Chauhan, N. Dhingra[34], R. Gupta, A. Kaur, A. Kaur, H. Kaur, M. Kaur, S. Kumar, P. Kumari, M. Meena, K. Sandeep, T. Sheokand, J.B. Singh[35], A. Singla, A. K. Virdi

University of Delhi, Delhi, India

A. Ahmed, A. Bhardwaj, A. Chhetri, B.C. Choudhary, A. Kumar, M. Naimuddin, K. Ranjan, S. Saumya

JHEP06(2023)060

Saha Institute of Nuclear Physics, HBNI, Kolkata, India

S. Baradia, S. Barman[36], S. Bhattacharya, D. Bhowmik, S. Dutta, S. Dutta, B. Gomber[37], M. Maity[36], P. Palit, G. Saha, B. Sahu, S. Sarkar

Indian Institute of Technology Madras, Madras, India

P.K. Behera, S.C. Behera, P. Kalbhor, J.R. Komaragiri[38], D. Kumar[38], A. Muhammad, L. Panwar[38], R. Pradhan, P.R. Pujahari, A. Sharma, A.K. Sikdar, P.C. Tiwari[38], S. Verma

Bhabha Atomic Research Centre, Mumbai, India

K. Naskar[39]

Tata Institute of Fundamental Research-A, Mumbai, India

T. Aziz, I. Das, S. Dugad, M. Kumar, G.B. Mohanty, P. Suryadevara

Tata Institute of Fundamental Research-B, Mumbai, India

S. Banerjee, R. Chudasama, M. Guchait, S. Karmakar, S. Kumar, G. Majumder, K. Mazumdar, S. Mukherjee, A. Thachayath

National Institute of Science Education and Research, An OCC of Homi Bhabha National Institute, Bhubaneswar, Odisha, India

S. Bahinipati[40], A.K. Das, C. Kar, P. Mal, T. Mishra, V.K. Muraleedharan Nair Bindhu[41], A. Nayak[41], P. Saha, S.K. Swain, D. Vats[41]

Indian Institute of Science Education and Research (IISER), Pune, India

A. Alpana, S. Dube, B. Kansal, A. Laha, S. Pandey, A. Rastogi, S. Sharma

Isfahan University of Technology, Isfahan, Iran

H. Bakhshiansohi[42,43], E. Khazaie[43], M. Zeinali[44]

Institute for Research in Fundamental Sciences (IPM), Tehran, Iran

S. Chenarani[45], S.M. Etesami, M. Khakzad, M. Mohammadi Najafabadi

University College Dublin, Dublin, Ireland

M. Grunewald

INFN Sezione di Bari[a], Università di Bari[b], Politecnico di Bari[c], Bari, Italy

M. Abbrescia[a,b], R. Aly[a,b,46], C. Aruta[a,b], A. Colaleo[a], D. Creanza[a,c], N. De Filippis[a,c], M. De Palma[a,b], A. Di Florio[a,b], W. Elmetenawee[a,b], F. Errico[a,b], L. Fiore[a], G. Iaselli[a,c], G. Maggi[a,c], M. Maggi[a], I. Margjeka[a,b], V. Mastrapasqua[a,b], S. My[a,b], S. Nuzzo[a,b], A. Pellecchia[a,b], A. Pompili[a,b], G. Pugliese[a,c], R. Radogna[a], D. Ramos[a], A. Ranieri[a], G. Selvaggi[a,b], L. Silvestris[a], F.M. Simone[a,b], Ü. Sözbilir[a], A. Stamerra[a], R. Venditti[a], P. Verwilligen[a]

JHEP06(2023)060

INFN Sezione di Bologna[a], Università di Bologna[b], Bologna, Italy
G. Abbiendi[a], C. Battilana[a,b], D. Bonacorsi[a,b], L. Borgonovi[a], R. Campanini[a,b], P. Capiluppi[a,b], A. Castro[a,b], F.R. Cavallo[a], C. Ciocca[a], M. Cuffiani[a,b], G.M. Dallavalle[a], T. Diotalevi[a,b], F. Fabbri[a], A. Fanfani[a,b], P. Giacomelli[a], L. Giommi[a,b], C. Grandi[a], L. Guiducci[a,b], S. Lo Meo[a,47], L. Lunerti[a,b], S. Marcellini[a], G. Masetti[a], F.L. Navarria[a,b], A. Perrotta[a], F. Primavera[a,b], A.M. Rossi[a,b], T. Rovelli[a,b], G.P. Siroli[a,b]

INFN Sezione di Catania[a], Università di Catania[b], Catania, Italy
S. Costa[a,b,48], A. Di Mattia[a], R. Potenza[a,b], A. Tricomi[a,b,48], C. Tuve[a,b]

INFN Sezione di Firenze[a], Università di Firenze[b], Firenze, Italy
G. Barbagli[a], G. Bardelli[a,b], B. Camaiani[a,b], A. Cassese[a], R. Ceccarelli[a,b], V. Ciulli[a,b], C. Civinini[a], R. D'Alessandro[a,b], E. Focardi[a,b], G. Latino[a,b], P. Lenzi[a,b], M. Lizzo[a,b], M. Meschini[a], S. Paoletti[a], R. Seidita[a,b], G. Sguazzoni[a], L. Viliani[a]

INFN Laboratori Nazionali di Frascati, Frascati, Italy
L. Benussi, S. Bianco, S. Meola[49], D. Piccolo

INFN Sezione di Genova[a], Università di Genova[b], Genova, Italy
M. Bozzo[a,b], P. Chatagnon[a], F. Ferro[a], E. Robutti[a], S. Tosi[a,b]

INFN Sezione di Milano-Bicocca[a], Università di Milano-Bicocca[b], Milano, Italy
A. Benaglia[a], G. Boldrini[a], F. Brivio[a,b], F. Cetorelli[a,b], F. De Guio[a,b], M.E. Dinardo[a,b], P. Dini[a], S. Gennai[a], A. Ghezzi[a,b], P. Govoni[a,b], L. Guzzi[a,b], M.T. Lucchini[a,b], M. Malberti[a], S. Malvezzi[a], A. Massironi[a], D. Menasce[a], L. Moroni[a], M. Paganoni[a,b], D. Pedrini[a], B.S. Pinolini[a], S. Ragazzi[a,b], N. Redaelli[a], T. Tabarelli de Fatis[a,b], D. Zuolo[a,b]

INFN Sezione di Napoli[a], Università di Napoli 'Federico II'[b], Napoli, Italy; Università della Basilicata[c], Potenza, Italy; Università G. Marconi[d], Roma, Italy
S. Buontempo[a], F. Carnevali[a,b], N. Cavallo[a,c], A. De Iorio[a,b], F. Fabozzi[a,c], A.O.M. Iorio[a,b], L. Lista[a,b,50], P. Paolucci[a,26], B. Rossi[a], C. Sciacca[a,b]

INFN Sezione di Padova[a], Università di Padova[b], Padova, Italy; Università di Trento[c], Trento, Italy
P. Azzi[a], N. Bacchetta[a,51], P. Bortignon[a], A. Bragagnolo[a,b], R. Carlin[a,b], P. Checchia[a], T. Dorigo[a], F. Gasparini[a,b], U. Gasparini[a,b], F. Gonella[a], G. Grosso[a], L. Layer[a,52], E. Lusiani[a], M. Margoni[a,b], A.T. Meneguzzo[a,b], J. Pazzini[a,b], P. Ronchese[a,b], R. Rossin[a,b], F. Simonetto[a,b], G. Strong[a], M. Tosi[a,b], H. Yarar[a,b], M. Zanetti[a,b], P. Zotto[a,b], A. Zucchetta[a,b], G. Zumerle[a,b]

JHEP06(2023)060

INFN Sezione di Pavia[a], Università di Pavia[b], Pavia, Italy

S. Abu Zeid[a,53], C. Aimè[a,b], A. Braghieri[a], S. Calzaferri[a,b], D. Fiorina[a,b], P. Montagna[a,b], V. Re[a], C. Riccardi[a,b], P. Salvini[a], I. Vai[a], P. Vitulo[a,b]

INFN Sezione di Perugia[a], Università di Perugia[b], Perugia, Italy

P. Asenov[a,54], G.M. Bilei[a], D. Ciangottini[a,b], L. Fanò[a,b], M. Magherini[a,b], G. Mantovani[a,b], V. Mariani[a,b], M. Menichelli[a], F. Moscatelli[a,54], A. Piccinelli[a,b], M. Presilla[a,b], A. Rossi[a,b], A. Santocchia[a,b], D. Spiga[a], T. Tedeschi[a,b]

INFN Sezione di Pisa[a], Università di Pisa[b], Scuola Normale Superiore di Pisa[c], Pisa, Italy; Università di Siena[d], Siena, Italy

P. Azzurri[a], G. Bagliesi[a], V. Bertacchi[a,c], R. Bhattacharya[a], L. Bianchini[a,b], T. Boccali[a], E. Bossini[a,b], D. Bruschini[a,c], R. Castaldi[a], M.A. Ciocci[a,b], V. D'Amante[a,d], R. Dell'Orso[a], M.R. Di Domenico[a,d], S. Donato[a], A. Giassi[a], F. Ligabue[a,c], G. Mandorli[a,c], D. Matos Figueiredo[a], A. Messineo[a,b], M. Musich[a,b], F. Palla[a], S. Parolia[a], G. Ramirez-Sanchez[a,c], A. Rizzi[a,b], G. Rolandi[a,c], S. Roy Chowdhury[a], T. Sarkar[a], A. Scribano[a], N. Shafiei[a,b], P. Spagnolo[a], R. Tenchini[a], G. Tonelli[a,b], N. Turini[a,d], A. Venturi[a], P.G. Verdini[a]

INFN Sezione di Roma[a], Sapienza Università di Roma[b], Roma, Italy

P. Barria[a], M. Campana[a,b], F. Cavallari[a], D. Del Re[a,b], E. Di Marco[a], M. Diemoz[a], E. Longo[a,b], P. Meridiani[a], G. Organtini[a,b], F. Pandolfi[a], R. Paramatti[a,b], C. Quaranta[a,b], S. Rahatlou[a,b], C. Rovelli[a], F. Santanastasio[a,b], L. Soffi[a], R. Tramontano[a,b]

INFN Sezione di Torino[a], Università di Torino[b], Torino, Italy; Università del Piemonte Orientale[c], Novara, Italy

N. Amapane[a,b], R. Arcidiacono[a,c], S. Argiro[a,b], M. Arneodo[a,c], N. Bartosik[a], R. Bellan[a,b], A. Bellora[a,b], C. Biino[a], N. Cartiglia[a], M. Costa[a,b], R. Covarelli[a,b], N. Demaria[a], M. Grippo[a,b], B. Kiani[a,b], F. Legger[a], C. Mariotti[a], S. Maselli[a], A. Mecca[a,b], E. Migliore[a,b], E. Monteil[a,b], M. Monteno[a], R. Mulargia[a], M.M. Obertino[a,b], G. Ortona[a], L. Pacher[a,b], N. Pastrone[a], M. Pelliccioni[a], M. Ruspa[a,c], K. Shchelina[a], F. Siviero[a,b], V. Sola[a], A. Solano[a,b], D. Soldi[a,b], A. Staiano[a], M. Tornago[a,b], D. Trocino[a], G. Umoret[a,b], A. Vagnerini[a,b]

INFN Sezione di Trieste[a], Università di Trieste[b], Trieste, Italy

S. Belforte[a], V. Candelise[a,b], M. Casarsa[a], F. Cossutti[a], A. Da Rold[a,b], G. Della Ricca[a,b], G. Sorrentino[a,b]

Kyungpook National University, Daegu, Korea

S. Dogra, C. Huh, B. Kim, D.H. Kim, G.N. Kim, J. Kim, J. Lee, S.W. Lee, C.S. Moon, Y.D. Oh, S.I. Pak, M.S. Ryu, S. Sekmen, Y.C. Yang

JHEP06(2023)060

Chonnam National University, Institute for Universe and Elementary Particles, Kwangju, Korea
H. Kim, D.H. Moon

Hanyang University, Seoul, Korea
E. Asilar, T.J. Kim, J. Park

Korea University, Seoul, Korea
S. Choi, S. Han, B. Hong, K. Lee, K.S. Lee, J. Lim, J. Park, S.K. Park, J. Yoo

Kyung Hee University, Department of Physics, Seoul, Korea
J. Goh

Sejong University, Seoul, Korea
H. S. Kim, Y. Kim, S. Lee

Seoul National University, Seoul, Korea
J. Almond, J.H. Bhyun, J. Choi, S. Jeon, J. Kim, J.S. Kim, S. Ko, H. Kwon, H. Lee, S. Lee, B.H. Oh, S.B. Oh, H. Seo, U.K. Yang, I. Yoon

University of Seoul, Seoul, Korea
W. Jang, D.Y. Kang, Y. Kang, D. Kim, S. Kim, B. Ko, J.S.H. Lee, Y. Lee, J.A. Merlin, I.C. Park, Y. Roh, D. Song, Watson, I.J., S. Yang

Yonsei University, Department of Physics, Seoul, Korea
S. Ha, H.D. Yoo

Sungkyunkwan University, Suwon, Korea
M. Choi, M.R. Kim, H. Lee, Y. Lee, Y. Lee, I. Yu

College of Engineering and Technology, American University of the Middle East (AUM), Dasman, Kuwait
T. Beyrouthy, Y. Maghrbi

Riga Technical University, Riga, Latvia
K. Dreimanis, G. Pikurs, A. Potrebko, M. Seidel, V. Veckalns

Vilnius University, Vilnius, Lithuania
M. Ambrozas, A. Carvalho Antunes De Oliveira, A. Juodagalvis, A. Rinkevicius, G. Tamulaitis

National Centre for Particle Physics, Universiti Malaya, Kuala Lumpur, Malaysia
N. Bin Norjoharuddeen, S.Y. Hoh[55], I. Yusuff[55], Z. Zolkapli

JHEP06(2023)060

Universidad de Sonora (UNISON), Hermosillo, Mexico

J.F. Benitez, A. Castaneda Hernandez, H.A. Encinas Acosta, L.G. Gallegos Maríñez, M. León Coello, J.A. Murillo Quijada, A. Sehrawat, L. Valencia Palomo

Centro de Investigacion y de Estudios Avanzados del IPN, Mexico City, Mexico

G. Ayala, H. Castilla-Valdez, I. Heredia-De La Cruz[56], R. Lopez-Fernandez, C.A. Mondragon Herrera, D.A. Perez Navarro, A. Sánchez Hernández

Universidad Iberoamericana, Mexico City, Mexico

C. Oropeza Barrera, F. Vazquez Valencia

Benemerita Universidad Autonoma de Puebla, Puebla, Mexico

I. Pedraza, H.A. Salazar Ibarguen, C. Uribe Estrada

University of Montenegro, Podgorica, Montenegro

I. Bubanja, J. Mijuskovic[57], N. Raicevic

National Centre for Physics, Quaid-I-Azam University, Islamabad, Pakistan

A. Ahmad, M.I. Asghar, A. Awais, M.I.M. Awan, M. Gul, H.R. Hoorani, W.A. Khan, M. Shoaib, M. Waqas

AGH University of Science and Technology Faculty of Computer Science, Electronics and Telecommunications, Krakow, Poland

V. Avati, L. Grzanka, M. Malawski

National Centre for Nuclear Research, Swierk, Poland

H. Bialkowska, M. Bluj, B. Boimska, M. Górski, M. Kazana, M. Szleper, P. Zalewski

Institute of Experimental Physics, Faculty of Physics, University of Warsaw, Warsaw, Poland

K. Bunkowski, K. Doroba, A. Kalinowski, M. Konecki, J. Krolikowski

Laboratório de Instrumentação e Física Experimental de Partículas, Lisboa, Portugal

M. Araujo, P. Bargassa, D. Bastos, C. Beirão Da Cruz E Silva, A. Boletti, P. Faccioli, M. Gallinaro, J. Hollar, N. Leonardo, T. Niknejad, M. Pisano, J. Seixas, J. Varela

VINCA Institute of Nuclear Sciences, University of Belgrade, Belgrade, Serbia

P. Adzic[58], M. Dordevic, P. Milenovic, J. Milosevic

JHEP06(2023)060

Centro de Investigaciones Energéticas Medioambientales y Tecnológicas (CIEMAT), Madrid, Spain

M. Aguilar-Benitez, J. Alcaraz Maestre, A. Álvarez Fernández, M. Barrio Luna, Cristina F. Bedoya, C.A. Carrillo Montoya, M. Cepeda, M. Cerrada, N. Colino, B. De La Cruz, A. Delgado Peris, D. Fernández Del Val, J.P. Fernández Ramos, J. Flix, M.C. Fouz, O. Gonzalez Lopez, S. Goy Lopez, J.M. Hernandez, M.I. Josa, J. León Holgado, D. Moran, C. Perez Dengra, A. Pérez-Calero Yzquierdo, J. Puerta Pelayo, I. Redondo, D.D. Redondo Ferrero, L. Romero, S. Sánchez Navas, J. Sastre, L. Urda Gómez, J. Vazquez Escobar, C. Willmott

Universidad Autónoma de Madrid, Madrid, Spain

J.F. de Trocóniz

Universidad de Oviedo, Instituto Universitario de Ciencias y Tecnologías Espaciales de Asturias (ICTEA), Oviedo, Spain

B. Alvarez Gonzalez, J. Cuevas, J. Fernandez Menendez, S. Folgueras, I. Gonzalez Caballero, J.R. González Fernández, E. Palencia Cortezon, C. Ramón Álvarez, V. Rodríguez Bouza, A. Soto Rodríguez, A. Trapote, C. Vico Villalba

Instituto de Física de Cantabria (IFCA), CSIC-Universidad de Cantabria, Santander, Spain

J.A. Brochero Cifuentes, I.J. Cabrillo, A. Calderon, J. Duarte Campderros, M. Fernandez, C. Fernandez Madrazo, A. García Alonso, G. Gomez, C. Lasaosa García, C. Martinez Rivero, P. Martinez Ruiz del Arbol, F. Matorras, P. Matorras Cuevas, J. Piedra Gomez, C. Prieels, A. Ruiz-Jimeno, L. Scodellaro, I. Vila, J.M. Vizan Garcia

University of Colombo, Colombo, Sri Lanka

M.K. Jayananda, B. Kailasapathy[59], D.U.J. Sonnadara, D.D.C. Wickramarathna

University of Ruhuna, Department of Physics, Matara, Sri Lanka

W.G.D. Dharmaratna, K. Liyanage, N. Perera, N. Wickramage

CERN, European Organization for Nuclear Research, Geneva, Switzerland

D. Abbaneo, J. Alimena, E. Auffray, G. Auzinger, J. Baechler, P. Baillon[†], D. Barney, J. Bendavid, M. Bianco, B. Bilin, A. Bocci, E. Brondolin, C. Caillol, T. Camporesi, G. Cerminara, N. Chernyavskaya, S.S. Chhibra, S. Choudhury, M. Cipriani, L. Cristella, D. d'Enterria, A. Dabrowski, A. David, A. De Roeck, M.M. Defranchis, M. Deile, M. Dobson, M. Dünser, N. Dupont, F. Fallavollita[60], A. Florent, L. Forthomme, G. Franzoni, W. Funk, S. Ghosh, S. Giani, D. Gigi, K. Gill, F. Glege, L. Gouskos, E. Govorkova, M. Haranko, J. Hegeman, V. Innocente, T. James, P. Janot, J. Kaspar, J. Kieseler, N. Kratochwil, S. Laurila, P. Lecoq, E. Leutgeb, C. Lourenço, B. Maier, L. Malgeri, M. Mannelli, A.C. Marini, F. Meijers, S. Mersi, E. Meschi, F. Moortgat, M. Mulders, S. Orfanelli,

JHEP06(2023)060

L. Orsini, F. Pantaleo, E. Perez, M. Peruzzi, A. Petrilli, G. Petrucciani, A. Pfeiffer, M. Pierini, D. Piparo, M. Pitt, H. Qu, T. Quast, D. Rabady, A. Racz, G. Reales Gutiérrez, M. Rovere, H. Sakulin, J. Salfeld-Nebgen, S. Scarfi, M. Selvaggi, A. Sharma, P. Silva, P. Sphicas[61], A.G. Stahl Leiton, S. Summers, K. Tatar, V.R. Tavolaro, D. Treille, P. Tropea, A. Tsirou, J. Wanczyk[62], K.A. Wozniak, W.D. Zeuner

Paul Scherrer Institut, Villigen, Switzerland

L. Caminada[63], A. Ebrahimi, W. Erdmann, R. Horisberger, Q. Ingram, H.C. Kaestli, D. Kotlinski, C. Lange, M. Missiroli[63], L. Noehte[63], T. Rohe

ETH Zurich - Institute for Particle Physics and Astrophysics (IPA), Zurich, Switzerland

T.K. Aarrestad, K. Androsov[62], M. Backhaus, P. Berger, A. Calandri, K. Datta, A. De Cosa, G. Dissertori, M. Dittmar, M. Donegà, F. Eble, M. Galli, K. Gedia, F. Glessgen, T.A. Gómez Espinosa, C. Grab, D. Hits, W. Lustermann, A.-M. Lyon, R.A. Manzoni, L. Marchese, C. Martin Perez, A. Mascellani[62], F. Nessi-Tedaldi, J. Niedziela, F. Pauss, V. Perovic, S. Pigazzini, M.G. Ratti, M. Reichmann, C. Reissel, T. Reitenspiess, B. Ristic, F. Riti, D. Ruini, D.A. Sanz Becerra, J. Steggemann[62], D. Valsecchi[26], R. Wallny

Universität Zürich, Zurich, Switzerland

C. Amsler[64], P. Bärtschi, C. Botta, D. Brzhechko, M.F. Canelli, K. Cormier, A. De Wit, R. Del Burgo, J.K. Heikkilä, M. Huwiler, W. Jin, A. Jofrehei, B. Kilminster, S. Leontsinis, S.P. Liechti, A. Macchiolo, P. Meiring, V.M. Mikuni, U. Molinatti, I. Neutelings, A. Reimers, P. Robmann, S. Sanchez Cruz, K. Schweiger, M. Senger, Y. Takahashi

National Central University, Chung-Li, Taiwan

C. Adloff[65], C.M. Kuo, W. Lin, P.K. Rout, S.S. Yu

National Taiwan University (NTU), Taipei, Taiwan

L. Ceard, Y. Chao, K.F. Chen, P.s. Chen, H. Cheng, W.-S. Hou, R. Khurana, G. Kole, Y.y. Li, R.-S. Lu, E. Paganis, A. Psallidas, A. Steen, H.y. Wu, E. Yazgan, P.r. Yu

Chulalongkorn University, Faculty of Science, Department of Physics, Bangkok, Thailand

C. Asawatangtrakuldee, N. Srimanobhas, V. Wachirapusitanand

Çukurova University, Physics Department, Science and Art Faculty, Adana, Turkey

D. Agyel, F. Boran, Z.S. Demiroglu, F. Dolek, I. Dumanoglu[66], E. Eskut, Y. Guler[67], E. Gurpinar Guler[67], C. Isik, O. Kara, A. Kayis Topaksu, U. Kiminsu, G. Onengut, K. Ozdemir[68], A. Polatoz, A.E. Simsek, B. Tali[69], U.G. Tok, S. Turkcapar, E. Uslan, I.S. Zorbakir

JHEP06(2023)060

Middle East Technical University, Physics Department, Ankara, Turkey
G. Karapinar[70], K. Ocalan[71], M. Yalvac[72]

Bogazici University, Istanbul, Turkey
B. Akgun, I.O. Atakisi, E. Gülmez, M. Kaya[73], O. Kaya[74], S. Tekten[75]

Istanbul Technical University, Istanbul, Turkey
A. Cakir, K. Cankocak[66], Y. Komurcu, S. Sen[76]

Istanbul University, Istanbul, Turkey
O. Aydilek, S. Cerci[69], B. Hacisahinoglu, I. Hos[77], B. Isildak[78], B. Kaynak, S. Ozkorucuklu, C. Simsek, D. Sunar Cerci[69]

Institute for Scintillation Materials of National Academy of Science of Ukraine, Kharkiv, Ukraine
B. Grynyov

National Science Centre, Kharkiv Institute of Physics and Technology, Kharkiv, Ukraine
L. Levchuk

University of Bristol, Bristol, United Kingdom
D. Anthony, E. Bhal, J.J. Brooke, A. Bundock, E. Clement, D. Cussans, H. Flacher, M. Glowacki, J. Goldstein, H.F. Heath, L. Kreczko, B. Krikler, S. Paramesvaran, S. Seif El Nasr-Storey, V.J. Smith, N. Stylianou[79], K. Walkingshaw Pass, R. White

Rutherford Appleton Laboratory, Didcot, United Kingdom
A.H. Ball, K.W. Bell, A. Belyaev[80], C. Brew, R.M. Brown, D.J.A. Cockerill, C. Cooke, K.V. Ellis, K. Harder, S. Harper, M.-L. Holmberg[81], Sh. Jain, J. Linacre, K. Manolopoulos, D.M. Newbold, E. Olaiya, D. Petyt, T. Reis, G. Salvi, T. Schuh, C.H. Shepherd-Themistocleous, I.R. Tomalin, T. Williams

Imperial College, London, United Kingdom
R. Bainbridge, P. Bloch, S. Bonomally, J. Borg, C.E. Brown, O. Buchmuller, V. Cacchio, V. Cepaitis, G.S. Chahal[82], D. Colling, J.S. Dancu, P. Dauncey, G. Davies, J. Davies, M. Della Negra, S. Fayer, G. Fedi, G. Hall, M.H. Hassanshahi, A. Howard, G. Iles, J. Langford, L. Lyons, A.-M. Magnan, S. Malik, A. Martelli, M. Mieskolainen, D.G. Monk, J. Nash[83], M. Pesaresi, B.C. Radburn-Smith, D.M. Raymond, A. Richards, A. Rose, E. Scott, C. Seez, R. Shukla, A. Tapper, K. Uchida, G.P. Uttley, L.H. Vage, T. Virdee[26], M. Vojinovic, N. Wardle, S.N. Webb, D. Winterbottom

Brunel University, Uxbridge, United Kingdom
K. Coldham, J.E. Cole, A. Khan, P. Kyberd, I.D. Reid

JHEP06(2023)060

Baylor University, Waco, Texas, U.S.A.

S. Abdullin, A. Brinkerhoff, B. Caraway, J. Dittmann, K. Hatakeyama, A.R. Kanuganti, B. McMaster, M. Saunders, S. Sawant, C. Sutantawibul, J. Wilson

Catholic University of America, Washington, DC, U.S.A.

R. Bartek, A. Dominguez, R. Uniyal, A.M. Vargas Hernandez

The University of Alabama, Tuscaloosa, Alabama, U.S.A.

S.I. Cooper, D. Di Croce, S.V. Gleyzer, C. Henderson, C.U. Perez, P. Rumerio[84], C. West

Boston University, Boston, Massachusetts, U.S.A.

A. Akpinar, A. Albert, D. Arcaro, C. Cosby, Z. Demiragli, C. Erice, E. Fontanesi, D. Gastler, S. May, J. Rohlf, K. Salyer, D. Sperka, D. Spitzbart, I. Suarez, A. Tsatsos, S. Yuan

Brown University, Providence, Rhode Island, U.S.A.

G. Benelli, B. Burkle, X. Coubez[21], D. Cutts, M. Hadley, U. Heintz, J.M. Hogan[85], T. Kwon, G. Landsberg, K.T. Lau, D. Li, J. Luo, M. Narain, N. Pervan, S. Sagir[86], F. Simpson, E. Usai, W.Y. Wong, X. Yan, D. Yu, W. Zhang

University of California, Davis, Davis, California, U.S.A.

J. Bonilla, C. Brainerd, R. Breedon, M. Calderon De La Barca Sanchez, M. Chertok, J. Conway, P.T. Cox, R. Erbacher, G. Haza, F. Jensen, O. Kukral, G. Mocellin, M. Mulhearn, D. Pellett, B. Regnery, Y. Yao, F. Zhang

University of California, Los Angeles, California, U.S.A.

M. Bachtis, R. Cousins, A. Datta, D. Hamilton, J. Hauser, M. Ignatenko, M.A. Iqbal, T. Lam, E. Manca, W.A. Nash, S. Regnard, D. Saltzberg, B. Stone, V. Valuev

University of California, Riverside, Riverside, California, U.S.A.

R. Clare, J.W. Gary, M. Gordon, G. Hanson, G. Karapostoli, O.R. Long, N. Manganelli, W. Si, S. Wimpenny

University of California, San Diego, La Jolla, California, U.S.A.

J.G. Branson, P. Chang, S. Cittolin, S. Cooperstein, D. Diaz, J. Duarte, R. Gerosa, L. Giannini, J. Guiang, R. Kansal, V. Krutelyov, R. Lee, J. Letts, M. Masciovecchio, F. Mokhtar, M. Pieri, B.V. Sathia Narayanan, V. Sharma, M. Tadel, E. Vourliotis, F. Würthwein, Y. Xiang, A. Yagil

University of California, Santa Barbara - Department of Physics, Santa Barbara, California, U.S.A.

N. Amin, C. Campagnari, M. Citron, G. Collura, A. Dorsett, V. Dutta, J. Incandela, M. Kilpatrick, J. Kim, A.J. Li, P. Masterson, H. Mei, M. Oshiro,

JHEP06(2023)060

M. Quinnan, J. Richman, U. Sarica, R. Schmitz, F. Setti, J. Sheplock, P. Siddireddy, D. Stuart, S. Wang

California Institute of Technology, Pasadena, California, U.S.A.

A. Bornheim, O. Cerri, I. Dutta, A. Latorre, J.M. Lawhorn, J. Mao, H.B. Newman, T. Q. Nguyen, M. Spiropulu, J.R. Vlimant, C. Wang, S. Xie, R.Y. Zhu

Carnegie Mellon University, Pittsburgh, Pennsylvania, U.S.A.

J. Alison, S. An, M.B. Andrews, P. Bryant, T. Ferguson, A. Harilal, C. Liu, T. Mudholkar, S. Murthy, M. Paulini, A. Roberts, A. Sanchez, W. Terrill

University of Colorado Boulder, Boulder, Colorado, U.S.A.

J.P. Cumalat, W.T. Ford, A. Hassani, G. Karathanasis, E. MacDonald, F. Marini, A. Perloff, C. Savard, N. Schonbeck, K. Stenson, K.A. Ulmer, S.R. Wagner, N. Zipper

Cornell University, Ithaca, New York, U.S.A.

J. Alexander, S. Bright-Thonney, X. Chen, D.J. Cranshaw, J. Fan, X. Fan, D. Gadkari, S. Hogan, J. Monroy, J.R. Patterson, D. Quach, J. Reichert, M. Reid, A. Ryd, J. Thom, P. Wittich, R. Zou

Fermi National Accelerator Laboratory, Batavia, Illinois, U.S.A.

M. Albrow, M. Alyari, G. Apollinari, A. Apresyan, L.A.T. Bauerdick, D. Berry, J. Berryhill, P.C. Bhat, K. Burkett, J.N. Butler, A. Canepa, G.B. Cerati, H.W.K. Cheung, F. Chlebana, K.F. Di Petrillo, J. Dickinson, V.D. Elvira, Y. Feng, J. Freeman, A. Gandrakota, Z. Gecse, L. Gray, D. Green, S. Grünendahl, D. Guerrero, O. Gutsche, R.M. Harris, R. Heller, T.C. Herwig, J. Hirschauer, L. Horyn, B. Jayatilaka, S. Jindariani, M. Johnson, U. Joshi, T. Klijnsma, B. Klima, K.H.M. Kwok, S. Lammel, D. Lincoln, R. Lipton, T. Liu, C. Madrid, K. Maeshima, C. Mantilla, D. Mason, P. McBride, P. Merkel, S. Mrenna, S. Nahn, J. Ngadiuba, D. Noonan, V. Papadimitriou, N. Pastika, K. Pedro, C. Pena[87], F. Ravera, A. Reinsvold Hall[88], L. Ristori, E. Sexton-Kennedy, N. Smith, A. Soha, L. Spiegel, J. Strait, L. Taylor, S. Tkaczyk, N.V. Tran, L. Uplegger, E.W. Vaandering, I. Zoi

University of Florida, Gainesville, Florida, U.S.A.

P. Avery, D. Bourilkov, L. Cadamuro, V. Cherepanov, R.D. Field, M. Kim, E. Koenig, J. Konigsberg, A. Korytov, E. Kuznetsova, K.H. Lo, K. Matchev, N. Menendez, G. Mitselmakher, A. Muthirakalayil Madhu, N. Rawal, D. Rosenzweig, S. Rosenzweig, K. Shi, J. Wang, Z. Wu

Florida State University, Tallahassee, Florida, U.S.A.

T. Adams, A. Askew, N. Bower, R. Habibullah, V. Hagopian, T. Kolberg, G. Martinez, H. Prosper, O. Viazlo, M. Wulansatiti, R. Yohay, J. Zhang

JHEP06(2023)060

Florida Institute of Technology, Melbourne, Florida, U.S.A.
M.M. Baarmand, S. Butalla, T. Elkafrawy[53], M. Hohlmann, R. Kumar Verma, M. Rahmani, F. Yumiceva

University of Illinois at Chicago (UIC), Chicago, Illinois, U.S.A.
M.R. Adams, H. Becerril Gonzalez, R. Cavanaugh, S. Dittmer, O. Evdokimov, C.E. Gerber, D.J. Hofman, D. S. Lemos, A.H. Merrit, C. Mills, G. Oh, T. Roy, S. Rudrabhatla, M.B. Tonjes, N. Varelas, X. Wang, Z. Ye, J. Yoo

The University of Iowa, Iowa City, Iowa, U.S.A.
M. Alhusseini, K. Dilsiz[89], L. Emediato, G. Karaman, O.K. Köseyan, J.-P. Merlo, A. Mestvirishvili[90], J. Nachtman, O. Neogi, H. Ogul[91], Y. Onel, A. Penzo, C. Snyder, E. Tiras[92]

Johns Hopkins University, Baltimore, Maryland, U.S.A.
O. Amram, B. Blumenfeld, L. Corcodilos, J. Davis, A.V. Gritsan, S. Kyriacou, P. Maksimovic, J. Roskes, S. Sekhar, M. Swartz, T.Á. Vámi

The University of Kansas, Lawrence, Kansas, U.S.A.
A. Abreu, L.F. Alcerro Alcerro, J. Anguiano, P. Baringer, A. Bean, Z. Flowers, T. Isidori, J. King, G. Krintiras, M. Lazarovits, C. Le Mahieu, C. Lindsey, J. Marquez, N. Minafra, M. Murray, M. Nickel, C. Rogan, C. Royon, R. Salvatico, S. Sanders, C. Smith, Q. Wang, G. Wilson

Kansas State University, Manhattan, Kansas, U.S.A.
B. Allmond, S. Duric, A. Ivanov, K. Kaadze, A. Kalogeropoulos, D. Kim, Y. Maravin, T. Mitchell, A. Modak, K. Nam, D. Roy

Lawrence Livermore National Laboratory, Livermore, California, U.S.A.
F. Rebassoo, D. Wright

University of Maryland, College Park, Maryland, U.S.A.
E. Adams, A. Baden, O. Baron, A. Belloni, A. Bethani, S.C. Eno, N.J. Hadley, S. Jabeen, R.G. Kellogg, T. Koeth, Y. Lai, S. Lascio, A.C. Mignerey, S. Nabili, C. Palmer, C. Papageorgakis, L. Wang, K. Wong

Massachusetts Institute of Technology, Cambridge, Massachusetts, U.S.A.
D. Abercrombie, W. Busza, I.A. Cali, Y. Chen, M. D'Alfonso, J. Eysermans, C. Freer, G. Gomez-Ceballos, M. Goncharov, P. Harris, M. Hu, D. Kovalskyi, J. Krupa, Y.-J. Lee, K. Long, C. Mironov, C. Paus, D. Rankin, C. Roland, G. Roland, Z. Shi, G.S.F. Stephans, J. Wang, Z. Wang, B. Wyslouch, T. J. Yang

University of Minnesota, Minneapolis, Minnesota, U.S.A.
R.M. Chatterjee, B. Crossman, A. Evans, J. Hiltbrand, B.M. Joshi, C. Kapsiak, M. Krohn, Y. Kubota, J. Mans, M. Revering, R. Rusack, R. Saradhy, N. Schroeder, N. Strobbe, M.A. Wadud

JHEP06(2023)060

University of Mississippi, Oxford, Mississippi, U.S.A.
L.M. Cremaldi

University of Nebraska-Lincoln, Lincoln, Nebraska, U.S.A.
K. Bloom, M. Bryson, D.R. Claes, C. Fangmeier, L. Finco, F. Golf, C. Joo, R. Kamalieddin, I. Kravchenko, I. Reed, J.E. Siado, G.R. Snow[†], W. Tabb, A. Wightman, F. Yan, A.G. Zecchinelli

State University of New York at Buffalo, Buffalo, New York, U.S.A.
G. Agarwal, H. Bandyopadhyay, L. Hay, I. Iashvili, A. Kharchilava, C. McLean, M. Morris, D. Nguyen, J. Pekkanen, S. Rappoccio, A. Williams

Northeastern University, Boston, Massachusetts, U.S.A.
G. Alverson, E. Barberis, Y. Haddad, Y. Han, A. Krishna, J. Li, J. Lidrych, G. Madigan, B. Marzocchi, D.M. Morse, V. Nguyen, T. Orimoto, A. Parker, L. Skinnari, A. Tishelman-Charny, T. Wamorkar, B. Wang, A. Wisecarver, D. Wood

Northwestern University, Evanston, Illinois, U.S.A.
S. Bhattacharya, J. Bueghly, Z. Chen, A. Gilbert, K.A. Hahn, Y. Liu, N. Odell, M.H. Schmitt, M. Velasco

University of Notre Dame, Notre Dame, Indiana, U.S.A.
R. Band, R. Bucci, M. Cremonesi, A. Das, R. Goldouzian, M. Hildreth, K. Hurtado Anampa, C. Jessop, K. Lannon, J. Lawrence, N. Loukas, L. Lutton, J. Mariano, N. Marinelli, I. Mcalister, T. McCauley, C. Mcgrady, K. Mohrman, C. Moore, Y. Musienko[11], R. Ruchti, A. Townsend, M. Wayne, H. Yockey, M. Zarucki, L. Zygala

The Ohio State University, Columbus, Ohio, U.S.A.
B. Bylsma, M. Carrigan, L.S. Durkin, B. Francis, C. Hill, M. Joyce, A. Lesauvage, M. Nunez Ornelas, K. Wei, B.L. Winer, B. R. Yates

Princeton University, Princeton, New Jersey, U.S.A.
F.M. Addesa, P. Das, G. Dezoort, P. Elmer, A. Frankenthal, B. Greenberg, N. Haubrich, S. Higginbotham, G. Kopp, S. Kwan, D. Lange, D. Marlow, I. Ojalvo, J. Olsen, D. Stickland, C. Tully

University of Puerto Rico, Mayaguez, Puerto Rico, U.S.A.
S. Malik, S. Norberg

Purdue University, West Lafayette, Indiana, U.S.A.
A.S. Bakshi, V.E. Barnes, R. Chawla, S. Das, L. Gutay, M. Jones, A.W. Jung, D. Kondratyev, A.M. Koshy, M. Liu, G. Negro, N. Neumeister, G. Paspalaki, S. Piperov, A. Purohit, J.F. Schulte, M. Stojanovic, J. Thieman, F. Wang, R. Xiao, W. Xie

JHEP06(2023)060

Purdue University Northwest, Hammond, Indiana, U.S.A.
J. Dolen, N. Parashar

Rice University, Houston, Texas, U.S.A.
D. Acosta, A. Baty, T. Carnahan, S. Dildick, K.M. Ecklund, P.J. Fernández Manteca, S. Freed, P. Gardner, F.J.M. Geurts, A. Kumar, W. Li, B.P. Padley, R. Redjimi, J. Rotter, S. Yang, E. Yigitbasi, L. Zhang[93], Y. Zhang

University of Rochester, Rochester, New York, U.S.A.
A. Bodek, P. de Barbaro, R. Demina, J.L. Dulemba, C. Fallon, T. Ferbel, M. Galanti, A. Garcia-Bellido, O. Hindrichs, A. Khukhunaishvili, P. Parygin, E. Popova, E. Ranken, R. Taus, G.P. Van Onsem

The Rockefeller University, New York, New York, U.S.A.
K. Goulianos

Rutgers, The State University of New Jersey, Piscataway, New Jersey, U.S.A.
B. Chiarito, J.P. Chou, Y. Gershtein, E. Halkiadakis, A. Hart, M. Heindl, D. Jaroslawski, O. Karacheban[24], I. Laflotte, A. Lath, R. Montalvo, K. Nash, M. Osherson, H. Routray, S. Salur, S. Schnetzer, S. Somalwar, R. Stone, S.A. Thayil, S. Thomas, H. Wang

University of Tennessee, Knoxville, Tennessee, U.S.A.
H. Acharya, A.G. Delannoy, S. Fiorendi, T. Holmes, E. Nibigira, S. Spanier

Texas A&M University, College Station, Texas, U.S.A.
O. Bouhali[94], M. Dalchenko, A. Delgado, R. Eusebi, J. Gilmore, T. Huang, T. Kamon[95], H. Kim, S. Luo, S. Malhotra, R. Mueller, D. Overton, D. Rathjens, A. Safonov

Texas Tech University, Lubbock, Texas, U.S.A.
N. Akchurin, J. Damgov, V. Hegde, K. Lamichhane, S.W. Lee, T. Mengke, S. Muthumuni, T. Peltola, I. Volobouev, A. Whitbeck

Vanderbilt University, Nashville, Tennessee, U.S.A.
E. Appelt, S. Greene, A. Gurrola, W. Johns, A. Melo, F. Romeo, P. Sheldon, S. Tuo, J. Velkovska, J. Viinikainen

University of Virginia, Charlottesville, Virginia, U.S.A.
B. Cardwell, B. Cox, G. Cummings, J. Hakala, R. Hirosky, A. Ledovskoy, A. Li, C. Neu, C.E. Perez Lara, B. Tannenwald

Wayne State University, Detroit, Michigan, U.S.A.
P.E. Karchin, N. Poudyal

JHEP06(2023)060

University of Wisconsin - Madison, Madison, Wisconsin, U.S.A.

S. Banerjee, K. Black, T. Bose, S. Dasu, I. De Bruyn, P. Everaerts, C. Galloni, H. He, M. Herndon, A. Herve, C.K. Koraka, A. Lanaro, A. Loeliger, R. Loveless, J. Madhusudanan Sreekala, A. Mallampalli, A. Mohammadi, S. Mondal, G. Parida, D. Pinna, A. Savin, V. Shang, V. Sharma, W.H. Smith, D. Teague, H.F. Tsoi, W. Vetens

Authors affiliated with an institute or an international laboratory covered by a cooperation agreement with CERN

S. Afanasiev, V. Andreev, Yu. Andreev, T. Aushev, M. Azarkin, A. Babaev, A. Belyaev, V. Blinov[96], E. Boos, V. Borshch, D. Budkouski, V. Bunichev, V. Chekhovsky, R. Chistov[96], M. Danilov[96], A. Dermenev, T. Dimova[96], I. Dremin, M. Dubinin[87], L. Dudko, V. Epshteyn, A. Ershov, G. Gavrilov, V. Gavrilov, S. Gninenko, V. Golovtcov, N. Golubev, I. Golutvin, I. Gorbunov, Y. Ivanov, V. Kachanov, L. Kardapoltsev[96], V. Karjavine, A. Karneyeu, V. Kim[96], M. Kirakosyan, D. Kirpichnikov, M. Kirsanov, V. Klyukhin, O. Kodolova, D. Konstantinov, V. Korenkov, A. Kozyrev[96], N. Krasnikov, A. Lanev, P. Levchenko, A. Litomin, N. Lychkovskaya, V. Makarenko, A. Malakhov, V. Matveev[96,97], V. Murzin, A. Nikitenko[98], S. Obraztsov, I. Ovtin[96], V. Palichik, V. Perelygin, M. Perfilov, S. Petrushanko, S. Polikarpov[96], V. Popov, O. Radchenko[96], M. Savina, V. Savrin, D. Selivanova, V. Shalaev, S. Shmatov, S. Shulha, Y. Skovpen[96], S. Slabospitskii, V. Smirnov, D. Sosnov, V. Sulimov, E. Tcherniaev, A. Terkulov, O. Teryaev, I. Tlisova, M. Toms, A. Toropin, L. Uvarov, A. Uzunian, E. Vlasov, A. Vorobyev, N. Voytishin, B.S. Yuldashev[99], A. Zarubin, I. Zhizhin, A. Zhokin

[†] *Deceased*
[1] *Also at TU Wien, Vienna, Austria*
[2] *Also at Institute of Basic and Applied Sciences, Faculty of Engineering, Arab Academy for Science, Technology and Maritime Transport, Alexandria, Egypt*
[3] *Also at Université Libre de Bruxelles, Bruxelles, Belgium*
[4] *Also at Universidade Estadual de Campinas, Campinas, Brazil*
[5] *Also at Federal University of Rio Grande do Sul, Porto Alegre, Brazil*
[6] *Also at UFMS, Nova Andradina, Brazil*
[7] *Also at University of Chinese Academy of Sciences, Beijing, China*
[8] *Also at Nanjing Normal University Department of Physics, Nanjing, China*
[9] *Now at The University of Iowa, Iowa City, Iowa, U.S.A.*
[10] *Also at University of Chinese Academy of Sciences, Beijing, China*
[11] *Also at an institute or an international laboratory covered by a cooperation agreement with CERN*
[12] *Also at Cairo University, Cairo, Egypt*
[13] *Also at Suez University, Suez, Egypt*
[14] *Now at British University in Egypt, Cairo, Egypt*
[15] *Also at Purdue University, West Lafayette, Indiana, U.S.A.*
[16] *Also at Université de Haute Alsace, Mulhouse, France*
[17] *Also at Department of Physics, Tsinghua University, Beijing, China*
[18] *Also at The University of the State of Amazonas, Manaus, Brazil*
[19] *Also at Erzincan Binali Yildirim University, Erzincan, Turkey*
[20] *Also at University of Hamburg, Hamburg, Germany*
[21] *Also at RWTH Aachen University, III. Physikalisches Institut A, Aachen, Germany*

JHEP06(2023)060

[22] Also at Isfahan University of Technology, Isfahan, Iran
[23] Also at Bergische University Wuppertal (BUW), Wuppertal, Germany
[24] Also at Brandenburg University of Technology, Cottbus, Germany
[25] Also at Forschungszentrum Jülich, Juelich, Germany
[26] Also at CERN, European Organization for Nuclear Research, Geneva, Switzerland
[27] Also at Physics Department, Faculty of Science, Assiut University, Assiut, Egypt
[28] Also at Karoly Robert Campus, MATE Institute of Technology, Gyongyos, Hungary
[29] Also at Wigner Research Centre for Physics, Budapest, Hungary
[30] Also at Institute of Physics, University of Debrecen, Debrecen, Hungary
[31] Also at Institute of Nuclear Research ATOMKI, Debrecen, Hungary
[32] Now at Universitatea Babes-Bolyai - Facultatea de Fizica, Cluj-Napoca, Romania
[33] Also at Faculty of Informatics, University of Debrecen, Debrecen, Hungary
[34] Also at Punjab Agricultural University, Ludhiana, India
[35] Also at UPES - University of Petroleum and Energy Studies, Dehradun, India
[36] Also at University of Visva-Bharati, Santiniketan, India
[37] Also at University of Hyderabad, Hyderabad, India
[38] Also at Indian Institute of Science (IISc), Bangalore, India
[39] Also at Indian Institute of Technology (IIT), Mumbai, India
[40] Also at IIT Bhubaneswar, Bhubaneswar, India
[41] Also at Institute of Physics, Bhubaneswar, India
[42] Also at Deutsches Elektronen-Synchrotron, Hamburg, Germany
[43] Now at Department of Physics, Isfahan University of Technology, Isfahan, Iran
[44] Also at Sharif University of Technology, Tehran, Iran
[45] Also at Department of Physics, University of Science and Technology of Mazandaran, Behshahr, Iran
[46] Also at Helwan University, Cairo, Egypt
[47] Also at Italian National Agency for New Technologies, Energy and Sustainable Economic Development, Bologna, Italy
[48] Also at Centro Siciliano di Fisica Nucleare e di Struttura Della Materia, Catania, Italy
[49] Also at Università degli Studi Guglielmo Marconi, Roma, Italy
[50] Also at Scuola Superiore Meridionale, Università di Napoli 'Federico II', Napoli, Italy
[51] Also at Fermi National Accelerator Laboratory, Batavia, Illinois, U.S.A.
[52] Also at Università di Napoli 'Federico II', Napoli, Italy
[53] Also at Ain Shams University, Cairo, Egypt
[54] Also at Consiglio Nazionale delle Ricerche - Istituto Officina dei Materiali, Perugia, Italy
[55] Also at Department of Applied Physics, Faculty of Science and Technology, Universiti Kebangsaan Malaysia, Bangi, Malaysia
[56] Also at Consejo Nacional de Ciencia y Tecnología, Mexico City, Mexico
[57] Also at IRFU, CEA, Université Paris-Saclay, Gif-sur-Yvette, France
[58] Also at Faculty of Physics, University of Belgrade, Belgrade, Serbia
[59] Also at Trincomalee Campus, Eastern University, Sri Lanka, Nilaveli, Sri Lanka
[60] Also at INFN Sezione di Pavia, Università di Pavia, Pavia, Italy
[61] Also at National and Kapodistrian University of Athens, Athens, Greece
[62] Also at Ecole Polytechnique Fédérale Lausanne, Lausanne, Switzerland
[63] Also at Universität Zürich, Zurich, Switzerland
[64] Also at Stefan Meyer Institute for Subatomic Physics, Vienna, Austria
[65] Also at Laboratoire d'Annecy-le-Vieux de Physique des Particules, IN2P3-CNRS, Annecy-le-Vieux, France
[66] Also at Near East University, Research Center of Experimental Health Science, Mersin, Turkey
[67] Also at Konya Technical University, Konya, Turkey
[68] Also at Izmir Bakircay University, Izmir, Turkey
[69] Also at Adiyaman University, Adiyaman, Turkey
[70] Also at Istanbul Gedik University, Istanbul, Turkey

JHEP06(2023)060

[71] *Also at Necmettin Erbakan University, Konya, Turkey*
[72] *Also at Bozok Universitetesi Rektörlügü, Yozgat, Turkey*
[73] *Also at Marmara University, Istanbul, Turkey*
[74] *Also at Milli Savunma University, Istanbul, Turkey*
[75] *Also at Kafkas University, Kars, Turkey*
[76] *Also at Hacettepe University, Ankara, Turkey*
[77] *Also at Istanbul University - Cerrahpasa, Faculty of Engineering, Istanbul, Turkey*
[78] *Also at Ozyegin University, Istanbul, Turkey*
[79] *Also at Vrije Universiteit Brussel, Brussel, Belgium*
[80] *Also at School of Physics and Astronomy, University of Southampton, Southampton, United Kingdom*
[81] *Also at University of Bristol, Bristol, United Kingdom*
[82] *Also at IPPP Durham University, Durham, United Kingdom*
[83] *Also at Monash University, Faculty of Science, Clayton, Australia*
[84] *Also at Università di Torino, Torino, Italy*
[85] *Also at Bethel University, St. Paul, Minnesota, U.S.A.*
[86] *Also at Karamanoğlu Mehmetbey University, Karaman, Turkey*
[87] *Also at California Institute of Technology, Pasadena, California, U.S.A.*
[88] *Also at United States Naval Academy, Annapolis, Maryland, U.S.A.*
[89] *Also at Bingol University, Bingol, Turkey*
[90] *Also at Georgian Technical University, Tbilisi, Georgia*
[91] *Also at Sinop University, Sinop, Turkey*
[92] *Also at Erciyes University, Kayseri, Turkey*
[93] *Also at Institute of Modern Physics and Key Laboratory of Nuclear Physics and Ion-beam Application (MOE) - Fudan University, Shanghai, China*
[94] *Also at Texas A&M University at Qatar, Doha, Qatar*
[95] *Also at Kyungpook National University, Daegu, Korea*
[96] *Also at another institute or international laboratory covered by a cooperation agreement with CERN*
[97] *Now at another institute or international laboratory covered by a cooperation agreement with CERN*
[98] *Also at Imperial College, London, United Kingdom*
[99] *Also at Institute of Nuclear Physics of the Uzbekistan Academy of Sciences, Tashkent, Uzbekistan*

JHEP06(2023)060